TECHNICAL RESEARCH REPORT

Computational Assessment of Suboptimal Bang-Bang Control Strategies for Performance-Based Design of Base Isolated Structures

by Robert Sebastianelli, Mark Austin

SEIL TR 2005-1
(ISR TR 2005-89)

Computational Assessment of

Suboptimal Bang-Bang Control Strategies for

Performance-Based Design of

Base Isolated Structures

By Robert R. Sebastianelli[1] and Mark Austin[2]

Last updated : June 20, 2005.

---

[1]Ph.D. Candidate, Department of Civil and Environmental Engineering, and Institute for Systems Research, University of Maryland, College Park, MD 20742, USA. E-mail : sebastn@isr.umd.edu

[2]Associate Professor, Department of Civil and Environmental Engineering, and Institute for Systems Research, University of Maryland, College Park, MD 20742, USA. E-mail : austin@isr.umd.edu

0

Contents

ABSTRACT

This paper explores the symbolic solution of the Lyapunov matrix equation as it applies to modified bang-bang control of base isolated structures. We present the Modified Bang-Bang Control strategy for active control of structures. Based on energy concepts, we formulate a rational choice of the "$\mathbf{Q}$" matrix that partitions the amount of potential energy in a base isolated system into two parts: (1) potential energy directed to the main structural system, and (2) potential energy directed to the isolation devices. This symbolic analysis of a 2-DOF system leads to investigating a choice of the $\mathbf{Q}$ matrix that minimizes the entire potential and/or kinetic energy of a n-DOF structure during an earthquake ground event. Using symbolic analyis procedures, We show that when the entire potential and/or kinetic energy of a n-DOF structure with uniform mass is minimized, solutions to the Lyapunov matrix equation assume a greatly simplified form. Moreover, this solution to the modified bang-bang control problem is easily calculated without needing to solve the Lyapunov matrix equation. Modified bang-bang control can be easily incorporated into the second-order differential equation of motion for the structure giving intuitive insight as to the effect of active control on the response of the structure. We show that this control strategy is insensititive to localized, nonlinear stiffness changes in the base isolators and therefore is well-suited for this problem area.

Chapter 1

Introduction

1.1 Problem Statement

For a wide range of moderate-to-large ground motion events, base isolated structures are expected to exhibit nonlinear displacement behavior at the isolator level, leaving the main structural system undamaged. Isolation devices are designed to have force-displacement characteristics that can survive hysteretic loadings without a loss in strength occuring. While the overall benefits of base isolation systems are well known [2, 3, 22, 29, 40, 39, 41], several vexing research issues remain to be resolved. For example, are there earthquakes whose ground motion characteristics make isolation an unsuitable option for design? Can the potential limitations and failure mechanisms of passive isolation (e.g., large deformation buckling of isolation devices; excessive lateral displacements in the isolator and main structural system) be mitigated with so-called hybrid passive-active isolation systems? Are passive-active isolation systems feasible? In a first step toward addressing these issues, researchers have proposed systems where the main isolation devices are supplemented by active control mechanisms. But this proposal, in itself, raises new questions! How, for example, does the selection of a control strategy propagate through to coefficients on displacement and velocity in the matrix product, $\mathbf{B}^\mathbf{T}\mathbf{S}z(t)$?

The scope of this study is restricted to passive base isolation systems supplemented by an active bang-bang control mechanism. While numerical algorithms exist for solving the Lyapunov matrix equation, systematic procedures for modeling base isolated structures, supplemented by bang-bang active control are still lacking [23]. For design purposes, we seek an analysis procedure that use performance-based metrics (e.g., displacements, velocities, energy) to capture the benefits of active control and base isolation, but is not overly complicated – indeed, we need to keep in mind that the complexity of the design method must be balanced against the uncertainity in ground motion prediction and in modeling of actual structural performance. On the structures side of the problem, recent research [5, 8, 9, 38]

1

suggests that overall input energy needs to be partitioned into two parts: (1) input energy directed to the main structural system, and (2) input energy directed tot the isolation devices. With respect to the active control, several strategies for implementation seem possible: (1) use a linear control theory, but iteratively adjust the structural parameters to account for the nonlinear behavior, (2) use a nonlinear control theory, or (3) use a linear control theory that has been shown to provide effective improvements to the system response, even when nonlinearities in behavior are not explicitly captured in the system model. Moreover, it is important to understand the sensitivity (and limitations) of modified bang-bang control to nonlinearities in the base isolated system because, for design purposes, it is a prerequisite to selection of an appropriate active control strategy.

Motivation for Supplementing Base Isolation with Active Control. Base isolation is one of the most successful methods for protecting structures against severe ground motions; however, due to the simplicity and passive nature of base isolation mechanisms, coupled with the unpredictable nature of future ground motions, base isolation is not a guareanteed means of effective protection for a wide range of seismic events [45]. One complicating factor is the sensitivity of "optimal designs" to localized site effects – an isolation system designed for a El Centro-type earthquake typically will not be optimal for a Northridge-type earthquake. Johnson et al. [24] and Spencer et al. [37] point out that recently there has been significant concern regarding the effectiveness of base isolation to protect structures against near-source, high-velocity, long-period pulse earthquakes. Such earthquake motions are difficult to accommodate. For example, a base isolated structure in one region of Los Angeles that may have readily survived the 1994 Northridge earthquake, may have well been destroyed if it were located elsewhere in the region [28]. Also, Housner et al. [23] and Reinhorn et al. [33] observe that since base isolation generally reduces the interstory drift and absolute acceleration of the structure at the expensive of large base displacement, the combination of active control with base isolation is able to achieve both low interstory drift, and at the same time, limit the maximum base displacement with a single set of control forces. Also, base isolated systems are limited in their ability to adapt to changing demands for structural response reduction. By supplementing base isolation with active control mechanisms, the hope is that higher levels of performance will be possible, and without a substantial increase in cost.

2

1.2 Equation of Motion

The well known general equation of motion for a multi-degree of freedom system subject to an earthquake load and external active controlling forces is as follows:

$$\mathbf{M}\ddot{x}(t) + \mathbf{C}\dot{x}(t) + \mathbf{K}x(t) = \mathbf{H}u(t) - \mathbf{M}r\ddot{x}_g(t). \tag{1.1}$$

In equation 1.1, $x(t)$ is a n-dimensional vector representing the relative displacements of the n degrees of freedom. $\mathbf{M}$, $\mathbf{C}$, and $\mathbf{K}$ are the mass, damping, and stiffness n x n matrices, repectively. $\ddot{x}_g(t)$ represents the earthquake ground acceleration, $\mathbf{H}$ is an n x p matrix that designates the location of the controller(s), while $u(t)$ is a p-dimensional vector that represents the control force of p-number of controllers.

The first-order differential equation, or state-space, form of equation 1.1 is given by the following:

$$\dot{z}(t) = \mathbf{A}z(t) + \mathbf{B}u(t) - \mathbf{W}\ddot{x}_g(t). \tag{1.2}$$

In equation 1.2,

$$z(t) = \begin{bmatrix} x(t) \\ \dot{x}(t) \end{bmatrix}; \tag{1.3}$$

$$\mathbf{A} = \begin{bmatrix} \mathbf{0} & \mathbf{1} \\ -\mathbf{M}^{-1}\mathbf{K} & -\mathbf{M}^{-1}\mathbf{C} \end{bmatrix}; \tag{1.4}$$

$$\mathbf{B} = \begin{bmatrix} \mathbf{0} \\ \mathbf{M}^{-1}\mathbf{H} \end{bmatrix}; \tag{1.5}$$

$$\mathbf{W} = \begin{bmatrix} 0 \\ r \end{bmatrix}. \tag{1.6}$$

1.3 Bang-Bang Control Law

One of the well-known control laws in optimal control theory is the bang-bang control law [11, 42, 43]. The key characteristic of optimal bang-bang control is a control force, $u(t)$, that switches from one extreme to another (i.e., the control force is always exerting its maximum force in either the positive or negative direction). Since the control force always takes on maximum values, the full capabilities

3

of the actuators can be exploited. Numerical simulation studies have shown that bang-bang control can provide better control efficiency than the well-known Linear Quadratic Regulator (LQR) Control Law [43].

Control Objective. The control objective for bang-bang control is to minimize:

$$J = \frac{1}{2} \int_0^{t_f} \left(z^T(t) \mathbf{Q} z(t) \right) dt. \tag{1.7}$$

where $z(t)$ is a $2n$ x 1 state vector of system displacements and velocities (for structural control, the state variables represent the displacements and velocities at the n-degrees of freedom), and $\mathbf{Q}$ is a positive semi-definite matrix whose content is left for the designer to choose. The well known optimal control solution [11, 42, 43] for a system in the form of equation 1.2 and which minimizes equation 1.7 is:

$$u(t) = -u_{max} \text{sgn} \left[\mathbf{B^T} \lambda(t) \right]; \tag{1.8}$$

where $\lambda(t)$ is known as the costate vector that is obtained by solving the following differential equation:

$$\dot{\lambda}(t) = -\mathbf{A^T} \lambda(t) - \mathbf{Q} z(t); \tag{1.9}$$

and u_{max} is a scalar that represents the maximum actuator control force. The other matrices in equations 1.8 and 1.9 are as previously defined. As part of the time history calculation of base isolated structures influenced by bang-bang active control, equation 1.9 must be solved at each timestep. Numerically stable integration algorithms such as the discrete implicit runge-kutta (DIRK2) method can be used to accomplish this task. Theoretical considerations can guide the selection of initial conditions for SDOF systems. However, for all other problems of practical importance, solutions to equation 1.9 are complicated by a lack of theoretical guidance for choosing the differential equation's initial conditions. An incorrect assumption (on the initial conditions) will lead to a numerical solution with time-varying characteristics that are correct, but is out of phase with the "correct optimal control solution." This may lead to an active controlled response that is worse than an uncontrolled response! We also note that the computational effort needed to solve 1.9 may be unwarrented, epecially when the considerable uncertainities associated with the modeling of seismically-resistant structures (e.g., ability to predict details of future ground motions, limitations of damping models) are taken into account.

1.4 Modified Bang-Bang Control Law

To avoid solving equation 1.9 at each time step for the entire time history response, a modified bang-bang control law is proposed by Wu and Soong [43].

Control Objective. Instead of minimizing equation 1.7, the objective of modified bang-bang control is to minimize the derivative of the following generalized energy function:

$$V[z(t)] = z^T(t)\mathbf{S}z(t). \tag{1.10}$$

Equation 1.10 is also referred to as the Lyapunov function, where the $\mathbf{S}$ matrix is the solution to the following Lyapunov matrix equation:

$$\mathbf{A^T S} + \mathbf{S A} = -\mathbf{Q}. \tag{1.11}$$

Taking the time derivative of equation 1.10 and substituting in the closed-loop state equation leads to the following equation results [25, 43]:

$$\dot{V}[z(t)] = -z^T(t)\mathbf{Q}z(t) + 2u^T(t)\mathbf{B^T S}z(t). \tag{1.12}$$

Close inspection of equation 1.12 indicates that in order for this equation to be a minimium for all possible state variables, $z(t)$, the second term on the right-hand side of equation 1.12 should result in a negative scalar for all possible $z(t)$, and moreover, $u(t)$ must be set to a maximum, say u_{max}. An appropriate choice for $u(t)$ that fullfills these two criteria is:

$$u(t) = -u_{max}\text{sgn}\left[\mathbf{B^T S}z(t)\right]. \tag{1.13}$$

This selection of $u(t)$ minimizes the derivative of the Lyapunov function at each time step, and hence, also minimizes the Lyaponov function itself (equation 1.12 at each time step of the response).

Equation of Motion. The effect of modified bang-bang control on the second-order differential equation of motion for a seismically-resistant structure is obtained by substituting equation 1.3 into equation 1.13, and then substituting the resultant equation into equation 1.1. The equation of motion is as follows:

$$\mathbf{M}\ddot{x}(t) + \mathbf{C}\dot{x}(t) + \mathbf{K}x(t) = -\mathbf{H}u_{max}\text{sgn}\left[\mathbf{B^T S}\left(\begin{array}{c} x(t) \\ \dot{x}(t) \end{array}\right)\right] - \mathbf{M}r\ddot{x}_g(t); \tag{1.14}$$

5

where the matrix, $\mathbf{S}$, is the $2n$ x $2n$ matrix solution to the Lyapunov matrix equation given in equation 1.11 and $\mathbf{B}$ is a $2n$ x p matrix as defined by equation 1.5.

For the remainder of this study, solutions to the Lyapunov equation for bang-bang control will be simply referred to as bang-bang control.

Observation Regarding the $\mathbf{B^T S}$ Matrix Product. Consider the matrix product $\mathbf{B^T S}$ for an n degree of freedom system. Since $\mathbf{B}$ has dimensions $2n$ x p and $\mathbf{S}$ has dimensions $2n$ x $2n$, the matrix product $\mathbf{B^T S}$ has dimensions p x $2n$. Since, by defination, the upper half of the $\mathbf{B}$ matrix is a n x p matrix of zeros, at most, only terms in rows $n + 1$ through $2n$ of $\mathbf{S}$ make any contribution to the matrix product $\mathbf{B^T S}$. We will employ this observation in our symbolic analysis of the inner workings for the bang-bang active control strategy.

1.5   Energy-Based Bang-Bang Control

From equations 1.11 and 1.13, it is evident that $\mathbf{Q}$ plays a central role in the bang-bang control strategy. It is therefore somewhat surprising that state-of-the-art procedures for structural control design tend to be ad hoc, letting iterative "trail and error" procedures and mathematical convenience drive the selection of terms in $\mathbf{Q}$ over first principles of engineering. While linear quadratic regulator (LQR) control is used extensively in control systems designed for structural control applications, the literature is scare in guidelines and justification for selection of design parameters $\mathbf{Q}$ (or $\mathbf{R}$). Kailath [25] (see page 219) states that the choice of the quantities is more of an art than science and is being further investigated. Both Belanger [10] (see pg. 305) and Connor [19] (see pg. 603) refer to perturbing terms in the weighing matrices until a desired result is obtained. Cai et al. [13] (see pg. 1653) uses the LQR method for comparison to their proposed sliding-mode bang-bang control method. In the LQR formulation, Cai et al.[13] sets the diagonal, elements of $\mathbf{Q}$ as relative, arbitary values, and the off-diagonal terms simply to zero.

A key tenet of our work is that the terms in $\mathbf{Q}$ should be selected so that the bang-bang control strategy has a well defined physical meaning. Wu, Soong, Gattulli, and Lin [44] suggest that under the LQR performance criteria, vibratory energy within the structure may be minimized by choosing $\mathbf{Q}$ to be one of the following options:

$$\mathbf{Q} = \begin{bmatrix} \mathbf{0} & \mathbf{0} \\ \mathbf{0} & \mathbf{M} \end{bmatrix} ; \mathbf{Q} = \begin{bmatrix} \mathbf{K} & \mathbf{0} \\ \mathbf{0} & \mathbf{0} \end{bmatrix} ; \mathbf{Q} = \begin{bmatrix} \mathbf{K} & \mathbf{0} \\ \mathbf{0} & \mathbf{M} \end{bmatrix} . \tag{1.15}$$

6

For the design of base isolated structures supplemented by active control, distributions of structural stiffness, together with system displacements, determine quantities of internal energy present within portions of the structure. A complicating factor is the heterogeneous role played by elements within the structure. While elements in the system superstructure are expected to remain essentially elastic (and, therefore, undamaged), the base isolation elements are expected to protect the superstructure by deforming well into the inelastic range without losing strength. To capture this duality, Austin [5, 8, 9] and Takewaki [38] suggest that overall input energy be partitioned into two parts: (1) input energy directed to the main structural system, and (2) input energy directed to the isolation devices. This energy-based approach to modified bang-bang control is valid because for the design of base isolated structures supplemented by active control, distributions of structural stiffness, together with system displacements, determine quantities of internal energy present within portions of the structure. Internal energy increases in proportion to the square of the displacements – hence, indirectly, internal energy is a measure of displacements, which in turn, is related to peak displacements and the likelihood of non-structural and structural damage. Models of structural performance need to capture force-displacement nonlinearities in the isolation devices.

1.5.1   Minimization of Superstructure Internal Energy

Since the relative displacement of the endpoints of a structural element are proportional to the square root of internal energy within the element, a reasonable control objective is minimization of the internal energy in the superstructure (i.e., everything except the base isolation devices).

Example 1. Internal Energy for the Superstructure of a Two Story Shear Structure. In mathematical terms, the internal energy in a single element of stiffness k is given by the following equation:

$$\text{Element I.E.(t)} = \frac{1}{2}k\left(x_2(t) - x_1(t)\right)^2 = \frac{1}{2}\begin{pmatrix} x_1(t), & x_2(t) \end{pmatrix}\begin{bmatrix} k & -k \\ -k & k \end{bmatrix}\begin{pmatrix} x_1(t) \\ x_2(t) \end{pmatrix}; \quad (1.16)$$

where $x_1(t)$ and $x_2(t)$ represent the end displacements of nodes 1 and 2, respectively. Now lets consider the 2-DOF system shown in Figure 1.1. The superstructure and base isolation systems have lateral stiffness k, and γk, respectively. Typically γ will lie in the interval 0.0-0.15. The internal energy of the superstructure (element 2) can be minimial by choosing $\mathbf{Q}$ as:
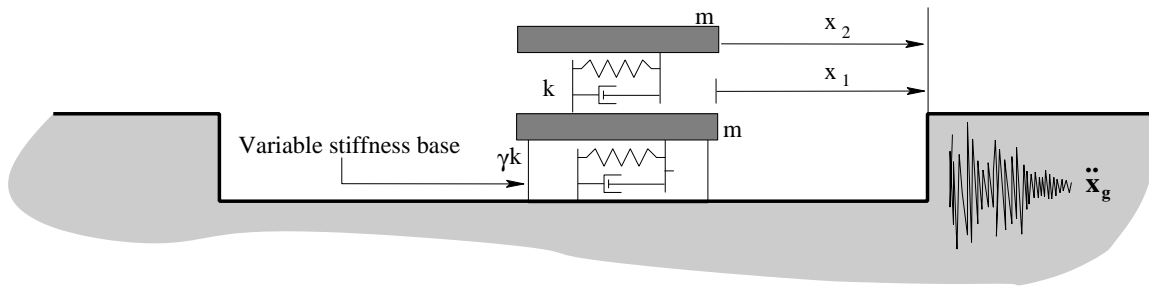
Figure 1.1: 2-DOF System

$$\mathbf{Q} = \begin{bmatrix} k & -k & 0 & 0 \\ -k & k & 0 & 0 \\ 0 & 0 & 0 & 0 \\ 0 & 0 & 0 & 0 \end{bmatrix}. \tag{1.17}$$

Substituting equation 1.17 into equation 1.7 and rearranging terms gives the following expression for J:

$$J = \frac{1}{2}k \int_0^{t_f} (x_1(t) - x_2(t))^2 \, dt; \tag{1.18}$$

which is simply the integral of the internal energy in element 2 over the time history of the structure.

For modified bang-bang control, substituting equation 1.17 into equation 1.12 leads to the following equation:

$$\dot{V}[z(t)] = k(x_1(t) - x_2(t))^2 + 2u^T(t)\mathbf{B^T S}z(t). \tag{1.19}$$

The first term on the right-hand side of equation 1.19 is an energy term corresponding to double the amount of internal energy in element 2 at any time, t. Physical considerations dictate that the second term on the right-hand side of equation 1.19 must also be in terms of energy. Since the actuator force, $u(t)$, is present in equation 1.19, this term may be thought of as the work done by the actuator force(s) on the structure at any time, t.

1.5.2 Base Isolator Internal Energy

Because base isolator elements are designed to exhibit nonlinear hysteretic behavior without a loss of strength occuring [1, 34, 36], large base displacements are expected during severe earthquake loadings. From a performance viewpoint, however, truly excessive lateral displacement of the isolator elements should be avoided because they can lead to localized buckling of the isolator devices and/or

8

collapse of the structure (details on the appropriate analysis procedures can be found in Naeim and Kelly [30]). Control of peak displacements must be balanced against a need for the base isolators to yield during an earthquake event and, therefore, do plastic work and dissipate energy. When the ground motions cease, ideally, permanent, plastic deformation of the isolator devices will be close to zero – indeed, we hope that the active control strategy and actuators will work towards this objective.

Example 2. Internal Base Isolator Energy for a Two Story Shear Structure. These performance criteria can be addressed indirectly through control of internal energy in the base isolators. Assuming that base isolators will be firmly attached to the ground (with full fixity), the internal energy is given by the following equation:

$$\text{Base Isolator Element Internal Energy(t)} = \frac{1}{2}\gamma k x_1(t)^2; \tag{1.20}$$

where γk is the lateral stiffness of the base isolator element and $x_1(t)$ represents the base isolator element degree of freedom that undergoes a displacement relative to the displacement of the ground. To minimize the internal energy in the base isolator (element 1) of the system shown in Figure 1.1, an appropriate choice for $\mathbf{Q}$ is:

$$\mathbf{Q} = \begin{bmatrix} \gamma k & 0 & 0 & 0 \\ 0 & 0 & 0 & 0 \\ 0 & 0 & 0 & 0 \\ 0 & 0 & 0 & 0 \end{bmatrix}. \tag{1.21}$$

Substituting equation 1.21 into equation 1.7 gives an expression for J that is the integral of the internal energy in the base isolator (element 1) over the time history of the structure.

For the modified bang-bang control case, substituting equation 1.21 into equation 1.12 gives an expression for $\dot{V}[z(t)]$ that represents the amount of internal energy in the base isolator (element 1) and a second energy term that represents the amount of work done on the structure by the actuator(s).

1.6   Research Objectives and Scope

Looking ahead, we envision performance-based design methods that will provide engineers with guidance in selecting appropriate control objectives and analysis procedures for base isolated buildings and bridges supplemented by active control. This vision is more likely to be realized if designers are provided with guidance on the performance capabilities/limitations and cause-and-effect relationships governing the active control.

In a departure from previous research efforts [5, 34, 36, 40, 39, 43], and in an attempt to bridge this gap, this study explores three avenues of investigation in the hope of better understanding the potential benefits of sub-optimal bang-bang control mechanisms as a supplement to performance-based design of base isolated structures. We are particularly interested in the role that symbolic and numerical analysis procedures associated with the Lyapunov equation can play. The research avenues are as follows:

1. **Symbolic Analysis For Single-Degree-of-Freedom Systems.** We explore the extent to which symbolic analysis can provide insight into the connection between an appropriate selection of $\mathbf{Q}$ and the active control strategy that follows through $\mathbf{B^T S} z(t)$. First, we use Mathematica$^{\copyright}$ to compute symbolic solutions to coefficients in $\mathbf{B^T S}$ for systems having one and two degrees of freedom. We will soon see that for structures having more than two-degrees of-freedom, the symbolic expressions are computationally intactable, even for Mathematica$^{\copyright}$.

2. **Symbolic Analysis For Multi-Degree-of-Freedom Systems.** Starting with relatively simple expressions for solutions to $\mathbf{B^T S}$, in a one degree of freedom structure, we determine the restrictions on the structural model that allow the solution to be scaled up to a n-DOF system.

3. **Sensitivity Analysis.** In the final part of this study, we explore the sensitivity of parameters in modified bang-bang control to localized nonlinear deformations in the base isolation devices.

The theoretical development of these research avenues is presented in Chapter 2. The principle outcome is matrices of symbolic expressions for bang-bang control (i.e., $\mathbf{B^T S}$) expressed in terms of the structural system parameters (i.e., m, k and c...) and state (i.e., displacements and velocities). In turn, the symbolic expressions allow for identification of: (1) The likely cause-and-effect relationships between details of the problem formulation and the time-history system response, and (2) The range of problem domains for which bang-bang control will be well defined. The purpose of Chapter 3 is to verify the performance aspects of these observations through numerical experiment. Time-history analyses are computed for a five-story based isolated structure, supplemented by bang-bang active control. Conclusions and future work are presented in Chapter 4.

Chapter 2

Symbolic Analysis

In this chapter we establish a theoretical foundation for the symbolic representation and sensitivity analysis of bang-bang control strategies tailored toward the nonlinear behavior and design of base isolated structures. We note that a key shortcoming in using numerical analysis packages to solve the Lyapunov equation for matrix $\mathbf{S}$, followed by the computation of $\mathbf{B^T S}z(t)$, is that any potential insight into the appropriate cause-and-effect relationships is buried inside the numerical procedure. To mitigate this shortcoming, in this chapter we explore the extent to which symbolic analysis procedures can provide insight into the connection between an appropriate selection of $\mathbf{Q}$ and the active control strategy that follows through $\mathbf{B^T S}z(t)$.

2.1 Linear Properties of the Lyapunov Matrix Equation

The multi-objective design of bang-bang control strategies is simplified by noting that for a given linear system, matrix $\mathbf{A}$ is fixed and matrix $\mathbf{S}$ is linearly dependent on $\mathbf{Q}$. In other words, given two Lyapunov matrix equations:

$$\mathbf{A^T S_1} + \mathbf{S_1 A} = \mathbf{Q_1}; \tag{2.1}$$

and

$$\mathbf{A^T S_2} + \mathbf{S_2 A} = \mathbf{Q_2}; \tag{2.2}$$

linearity of the Lyapunov matrix equations with respect to $\mathbf{S}$ implies:

$$\mathbf{A^T} \left(a\mathbf{S_1} + b\mathbf{S_2} \right) + \left(a\mathbf{S_1} + b\mathbf{S_2} \right) \mathbf{A} = a\mathbf{Q_1} + b\mathbf{Q_2}. \tag{2.3}$$

where a and b are arbitrary coefficients. A proof of the linear matrix properties of the Lyapunov matrix equation is given by Belanger [10].

We envision that in a performance-based approach to design, a designer will select parameters "a" and "b" in a manner that reflects the importance of minimizing the potential energy in the base isolators and superstructure, respectively. Trade-offs between our two control objectives may be easily investigated by solving equation 2.3 with $a = 1$ and $b = 0$ and with $a = 0$ and $b = 1$. The solution matrices $\mathbf{S_1}$ and $\mathbf{S_2}$ may be scaled to obtained any desired combination of a and b.

2.2 Research Avenue 1. Symbolic Analysis of Single-Degree-of-Freedom Systems

In this section we use Mathematica$^{\copyright}$ to compute a symbolic solution to coefficients in $\mathbf{B^T S}$ for a one degree of freedom system. We then investigate the circumstances under which the bang-bang control force will change sign, and prove that under a damped steady state system response, the bang-bang control is neither perfectly in phase with the displacements nor velocities.

2.2.1 Symbolic Representation for 1-DOF Bang-Bang Control Strategy

Consider a 1-DOF system with stiffness, k, mass, m, and damping, c$= \alpha \cdot m + \beta \cdot k$. Assume that the 1-DOF system has an actuator acting on the DOF. For the following general choice of $\mathbf{Q}$,

$$\mathbf{Q} = \left[\begin{array}{cc} k^\star & 0 \\ 0 & 0 \end{array} \right], \tag{2.4}$$

where $k^\star$ is a real, positive number, the symbolic representation for the $\mathbf{B^T S}$ matrix product, as determined by Mathematica$^{\copyright}$ is as follows:

$$\mathbf{B^T S} = \left[\begin{array}{cc} 0 & \frac{1}{m} \end{array} \right] \left[\begin{array}{cc} \frac{mk^\star}{2(\alpha \cdot m + \beta \cdot k)} + \frac{(\alpha \cdot m + \beta \cdot k)k^\star}{2k} & \frac{mk^\star}{2k} \\ \frac{mk^\star}{2k} & \frac{m^2 k^\star}{2k(\alpha \cdot m + \beta \cdot k)} \end{array} \right] = \left[\begin{array}{cc} \frac{k^\star}{2k} & \frac{mk^\star}{2k(\alpha \cdot m + \beta \cdot k)} \end{array} \right]. \tag{2.5}$$

When the terms in $\mathbf{Q}$ are selected to minimize potential energy in the 1-DOF system (i.e., $k^\star = k$), equation 2.5 simplifies to:

$$\mathbf{B^T S} = \left[\begin{array}{cc} 0 & \frac{1}{m} \end{array} \right] \left[\begin{array}{cc} \frac{mk}{2(\alpha \cdot m + \beta \cdot k)} + \frac{\alpha \cdot m + \beta \cdot k}{2} & \frac{m}{2} \\ \frac{m}{2} & \frac{m^2}{2(\alpha \cdot m + \beta \cdot k)} \end{array} \right] = \left[\begin{array}{cc} \frac{1}{2} & \frac{m}{2(\alpha \cdot m + \beta \cdot k)} \end{array} \right]. \tag{2.6}$$

12

Similiarly, when

$$\mathbf{Q} = \begin{bmatrix} 0 & 0 \\ 0 & m^{\star} \end{bmatrix}, \tag{2.7}$$

where $m^{\star}$ is a real, positive number, the $\mathbf{B^T S}$ matrix product was calculated symbolically using Mathematica©
as:

$$\mathbf{B^T S} = \begin{bmatrix} 0 & \frac{1}{m} \end{bmatrix} \begin{bmatrix} \frac{m^{\star}k}{2(\alpha \cdot m + \beta \cdot k)} & 0 \\ 0 & \frac{mm^{\star}}{2(\alpha \cdot m + \beta \cdot k)} \end{bmatrix} = \begin{bmatrix} 0 & \frac{m^{\star}}{2(\alpha \cdot m + \beta \cdot k)} \end{bmatrix}. \tag{2.8}$$

If the kinetic energy, $T(\dot{x}(t))$, in this 1-DOF system is minimized, i.e., $m^{\star} = m$, equation 2.8 becomes:

$$\mathbf{B^T S} = \begin{bmatrix} 0 & \frac{1}{m} \end{bmatrix} \begin{bmatrix} \frac{mk}{2(\alpha \cdot m + \beta \cdot k)} & 0 \\ 0 & \frac{m^2}{2(\alpha \cdot m + \beta \cdot k)} \end{bmatrix} = \begin{bmatrix} 0 & \frac{m}{2(\alpha \cdot m + \beta \cdot k)} \end{bmatrix}. \tag{2.9}$$

Due to the linear properties of the Lyapunov matrix equation, the $\mathbf{B^T S}$ matrix product that minimizes
the total (potential + kinetic) energy of this 1-DOF system is the sum of equations 2.6 and 2.9.

2.2.2   Effectiveness of Bang-Bang Control in a 1-DOF System

In this section we investigate the effectiveness of bang-bang control in the situation of a linearly
elastic 1-DOF system subject to a simplified ground motion. Initially, we assume: (1) the ground motion
can be modeled as a periodic forcing function, and (2) steady state system response. Then in part two,
we look at the effectiveness of bang-bang control when the 1-DOF system is in transient free vibration.
We prove that the actuator works neither perfectly in phase with displacements nor perfectly in phase
with velocities.

Steady State Response

Let us assume that the forcing function due to ground accelerations is:

$$p(g, t) = A\sin(gt) \tag{2.10}$$

where "g" matches the "most dominant" natural circular frequency for ground shaking. If $\beta = (g/w)$
then the steady-state displacement and velocity are [15]:

$$x(t) = \begin{bmatrix} \frac{A}{k} \end{bmatrix} \cdot \begin{bmatrix} \frac{(1 - \beta^2)\sin(gt) - 2\xi\beta\cos(gt)}{(1 - \beta^2)^2 + (2\xi\beta)^2} \end{bmatrix} \tag{2.11}$$

13

and

$$\dot{x}(t) = \left[\frac{Ag}{k}\right] \cdot \left[\frac{(1 - \beta^2)\cos(gt) + 2\xi\beta\sin(gt)}{(1 - \beta^2)^2 + (2\xi\beta)^2}\right]. \tag{2.12}$$

Amplitude of Response. From the triginometric identity,

$$\sin(gt + \phi) = \sin(gt) \cdot \cos(\phi) + \cos(gt) \cdot \sin(\phi) \tag{2.13}$$

it follows that equation 2.11 can be written,

$$x(t) = \left[\frac{A}{k}\right] \cdot \left[\frac{1}{(1 - \beta^2)^2 + (2\xi\beta)^2}\right] \cdot \sin(gt + \phi) \tag{2.14}$$

where

$$\tan(\phi) = \left[\frac{-2\xi\beta}{(1 - \beta^2)}\right]. \tag{2.15}$$

The amplitude of the displacement vector is:

$$\|x(t)\| = \left[\frac{A}{k}\right] \cdot \left[\frac{1}{(1 - \beta^2)^2 + (2\xi\beta)^2}\right]. \tag{2.16}$$

Similarly, the amplitude of the velocity vector is:

$$\|\dot{x}(t)\| = \left[\frac{Ag}{k}\right] \cdot \left[\frac{1}{(1 - \beta^2)^2 + (2\xi\beta)^2}\right]. \tag{2.17}$$

Bang-Bang Control Strategy. When the terms in $\mathbf{Q}$ are selected to minimize potential energy in the 1-DOF system (i.e., $k^\star = k$), the matrix product $B^T S$ simplifies to:

$$\mathbf{B^T S} = \begin{bmatrix} 0 & \frac{1}{m} \end{bmatrix} \begin{bmatrix} \frac{mk}{2(\alpha \cdot m + \beta \cdot k)} + \frac{\alpha \cdot m + \beta \cdot k}{2} & \frac{m}{2} \\ \frac{m}{2} & \frac{m^2}{2(\alpha \cdot m + \beta \cdot k)} \end{bmatrix} = \begin{bmatrix} \frac{1}{2} & \frac{m}{2(\alpha \cdot m + \beta \cdot k)} \end{bmatrix}. \tag{2.18}$$

Substituting equations 2.11 and 2.12 into $\mathbf{Z}(t) = [x(t), \dot{x}(t)]^T$ and pre-multiplying by equation 2.18 gives:

$$\mathbf{B^T SZ} = \left[\frac{A}{2k}\right] \cdot \left[\frac{(1 - \beta^2)\sin(gt) - 2\xi\beta\cos(gt) + \frac{mg}{c}(1 - \beta^2)\cos(gt) + \frac{2mg}{c}\xi\beta\sin(gt)}{(1 - \beta^2)^2 + (2\xi\beta)^2}\right] \tag{2.19}$$

14

Amplitude of Displacement and Velocity Contributions. The amplitude of displacement and velocity terms in equation 2.19 is:

$$\| \quad \text{displacement component}(t) \quad \| = \left[\frac{A}{2k}\right] \cdot \left[\frac{1}{(1-\beta^2)^2 + (2\xi\beta)^2}\right] \qquad (2.20)$$

and

$$\| \quad \text{velocity component}(t) \quad \| = \left[\frac{Amg}{2ck}\right] \cdot \left[\frac{1}{(1-\beta^2)^2 + (2\xi\beta)^2}\right]. \qquad (2.21)$$

Notice that as $c \to 0$, the velocity component amplitude increases in size relative to the amplitude of the displacement term.

Strategy for Switching Direction of the Actuator Force. From the viewpoint of bang-bang control we want to know in which direction the actuator will push as a function of the displacement/velocity state variables, and how the strategy varies as a function of the problem parameters. The actuator will switch directions in the force application when:

$$(1-\beta^2)\sin(gt) - 2\xi\beta\cos(gt) + \frac{mg}{c}(1-\beta^2)\cos(gt) + \frac{2mg}{c}\xi\beta\sin(gt) = 0. \qquad (2.22)$$

Collecting and rearranging common terms:

$$\left[(1-\beta^2) + \frac{2mg}{c}\xi\beta\right]\sin(gt) = \left[2\xi\beta - \frac{mg}{c}(1-\beta^2)\right]\cos(gt) \qquad (2.23)$$

gives:

$$\tan(gt) = \left[\frac{\left[2\xi\beta - \frac{mg}{c}(1-\beta^2)\right]}{\left[(1-\beta^2) + \frac{2mg}{c}\xi\beta\right]}\right]. \qquad (2.24)$$

Now recall that $\xi = c/2mw$ and $\beta = g/w$. The expression,

$$\frac{2mg}{c}\xi\beta \qquad \text{simplifies to...} \qquad \beta^2, \qquad (2.25)$$

and

$$\frac{mg}{c}(1-\beta^2) \qquad \text{can be re-written as...} \qquad \frac{\beta}{2\xi} \cdot (1-\beta^2). \qquad (2.26)$$

Hence, equation 2.24 simplifies to:

$$\tan(gt) = \left[2\xi\beta - \frac{\beta}{2\xi} \cdot (1 - \beta^2) \right] \tag{2.27}$$

Case 1. The actuator works perfactly in phase with displacements when a change in actuator force and displacements occurs at the same time. From equation 2.11, x(t) = 0 when:

$$(1 - \beta^2)\sin(gt) - 2\xi\beta\cos(gt) = 0. \tag{2.28}$$

i.e.,

$$\tan(gt) = \left[\frac{2\xi\beta}{(1 - \beta^2)} \right] \tag{2.29}$$

Case 2. The actuator works perfactly in phase with velocities – i.e., to oppose the direction of motion – when $\dot{x}$(t) = 0. i.e.,

$$(1 - \beta^2)\cos(gt) + 2\xi\beta\sin(gt) = 0. \tag{2.30}$$

i.e.,

$$\tan(gt) = \left[\frac{(\beta^2 - 1)}{2\xi\beta} \right] \tag{2.31}$$

Theorem 1. For values of $\beta \neq 0$, the actuator works neither perfectly in phase with displacements nor perfectly in phase with velocities.

Proof. From equations 2.27 and 2.29 it is evident that in order for the actuator to work perfectly in phase with displacements we require:

$$\frac{2\xi\beta}{(1 - \beta^2)} = \left[2\xi\beta - \frac{\beta}{2\xi} \cdot (1 - \beta^2) \right] \tag{2.32}$$

The trivial ... and not very useful ... solution is $\beta = 0$. Rearranging the remaining terms gives,

$$\xi^2 = \left[\frac{-(1 - \beta^2)^2}{4\beta^2} \right]. \tag{2.33}$$

Physical considerations dictate that ξ must be greater than zero (i.e., we want the bang-bang control strategy and damping in the physical system to be well defined). From equation 2.33 it is evident,
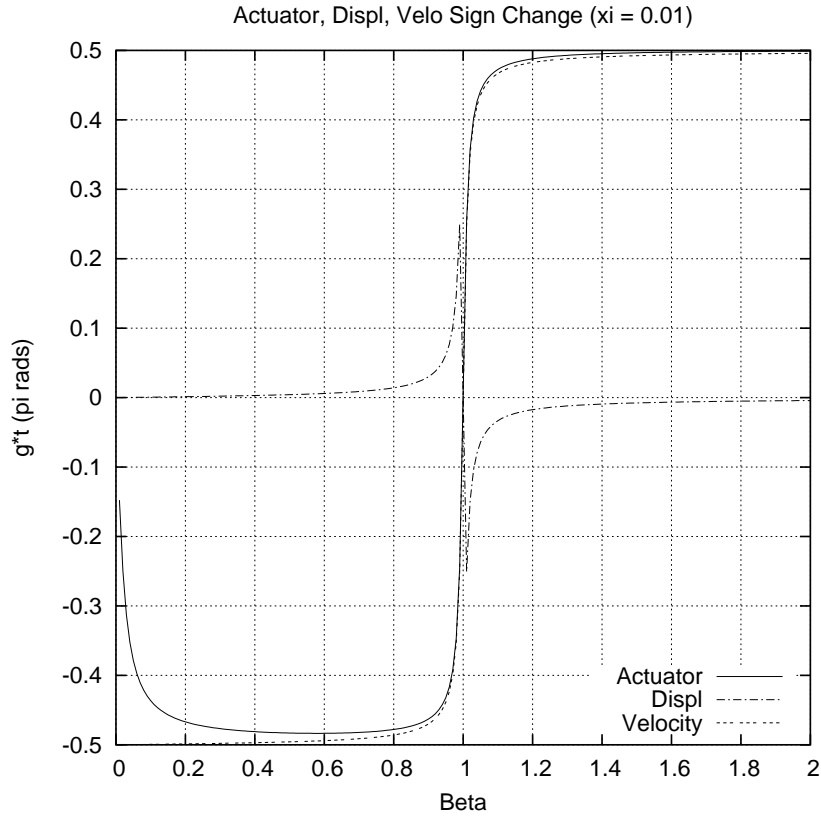
Figure 2.1: Actuator, Displacement, and Velocity Sign Change ($\xi = 0.01$)

however, that no value of β exists for which this will occur. The left- and right-hand sides of equation 2.33 will be closest in value when $\beta = 1$ and $\gamma \approx 0$ (i.e., a very lightly damped system is forced near its resonance frequency).

Similarly, in order for the actuator to work perfectly in phase with velocities we require:

$$\frac{(\beta^2 - 1)}{2\xi\beta} = \left[2\xi\beta - \frac{\beta}{2\xi} \cdot (1 - \beta^2)\right] \tag{2.34}$$

Rearranging terms gives,

$$\xi^2 = \left[\frac{(\beta^2 - 1)(1 - \beta^2)}{4\beta^2}\right] = \left[\frac{-(1 - \beta^2)^2}{4\beta^2}\right]. \tag{2.35}$$

There are no values of β, including $\beta = 0$, which will make make the right-hand side of equation 2.35 positive.

Plots of Phase Shift vs Beta

17

Figures 2.1 through 2.3 show the phase shift in displacements, velocities and actuator force change as a function of β for contours of damping, $\xi = 0.01$, $\xi = 0.05$ and $\xi = 0.09$, respectively. Notice that the contours of displacement and velocity phase shift are separated by $\pi/2$ radians. Moreover, as predicted by the theorem, phase shift for the bang-bang control is synchronized with displaacement phase shift at only two points – $\beta = 0$ and 1. What the mathematics doesn't show is that bang-bang control is "almost in phase" with velocities for β values covering the interval 0.8 through 1.2.

Free Vibration Response

Now let us assume that the ground acceleration ceases and the structure enters a free vibration response,

$$x(t) = e^{-\xi w_o t} \left[A \cos(w_d t) + B \sin(w_d t) \right] \tag{2.36}$$

with initial displacement and velocity $x(0)$ and $\dot{x}(0)$, respectively. The time history of displacement and velocity are,

$$x(t) = e^{-\xi w_o t} \left[x(0) \cos(w_d t) + \frac{\dot{x}(0) + x(0)\xi w_o}{w_d} \sin(w_d t) \right] \tag{2.37}$$

and

$$\dot{x}(t) = e^{-\xi w_o t} \left[\dot{x}(0) \cos(w_d t) - \frac{1}{\sqrt{1 - \xi^2}} \left(\xi \dot{x}(0) + (\xi + \sqrt{1 - \xi^2}) w_o x(0) \right) \sin(w_d t) \right]. \tag{2.38}$$

Bang-Bang Control Strategy. Substituting equations 2.37 and 2.38 into $\mathbf{Z}(t) = [x(t), \dot{x}(t)]^T$ and pre-multiplying by equation 2.18 gives:

$$\mathbf{B^T S Z} = \left[\frac{1}{2} \right] x(t) + \left[\frac{m}{2c} \right] \dot{x}(t) = \left[\frac{1}{2} \right] \left[x(t) + \frac{1}{2\xi w} \dot{x}(t) \right]. \tag{2.39}$$

Strategy for Switching Direction of the Actuator Force. The actuator will switch directions in the force application when:

$$C \cos(w_d t) + D \sin(w_d t) = 0, \tag{2.40}$$

where

$$C = \frac{x(0)}{2} + \frac{\dot{x}(0)}{4\xi w_o} \tag{2.41}$$

18
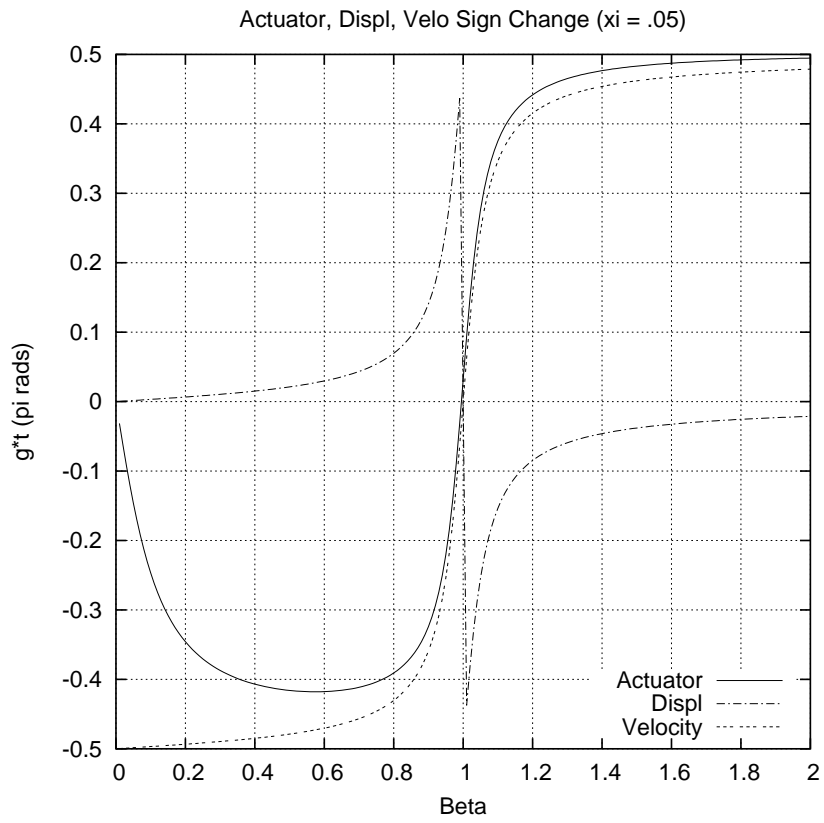
Figure 2.2: Actuator, Displacement, and Velocity Sign Change ($\xi = 0.05$)

19
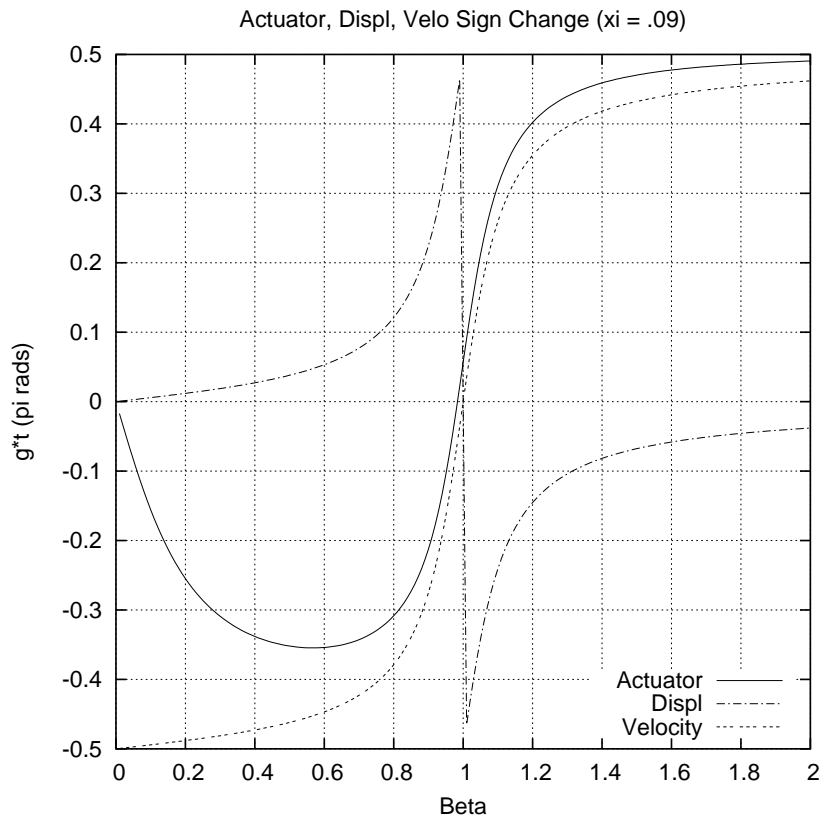
Figure 2.3: Actuator,Displacement, and Velocity Sign Change ($\xi = 0.09$)
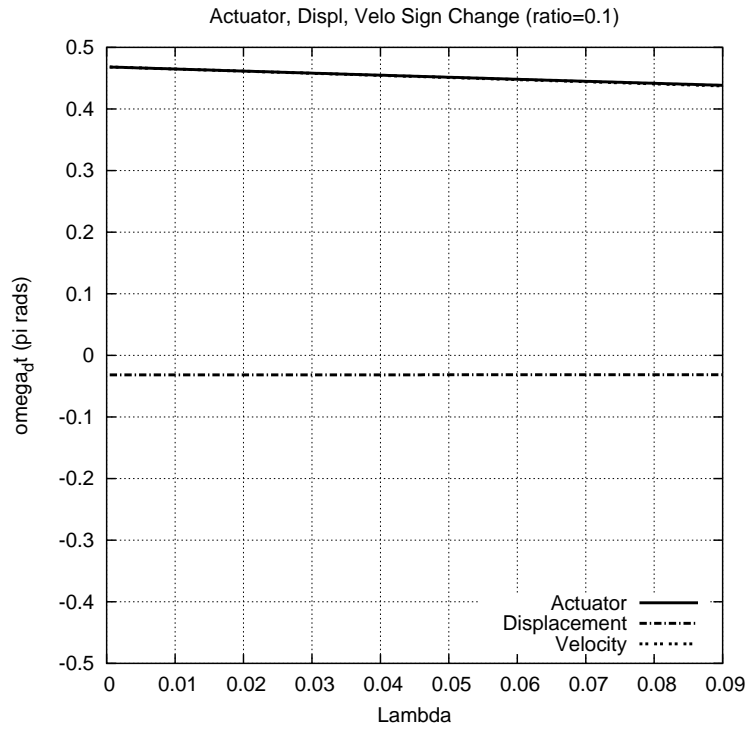
Figure 2.4: Actuator, Displacement, and Velocity Sign Change During Free Vibration ($\rho = 0.1$)
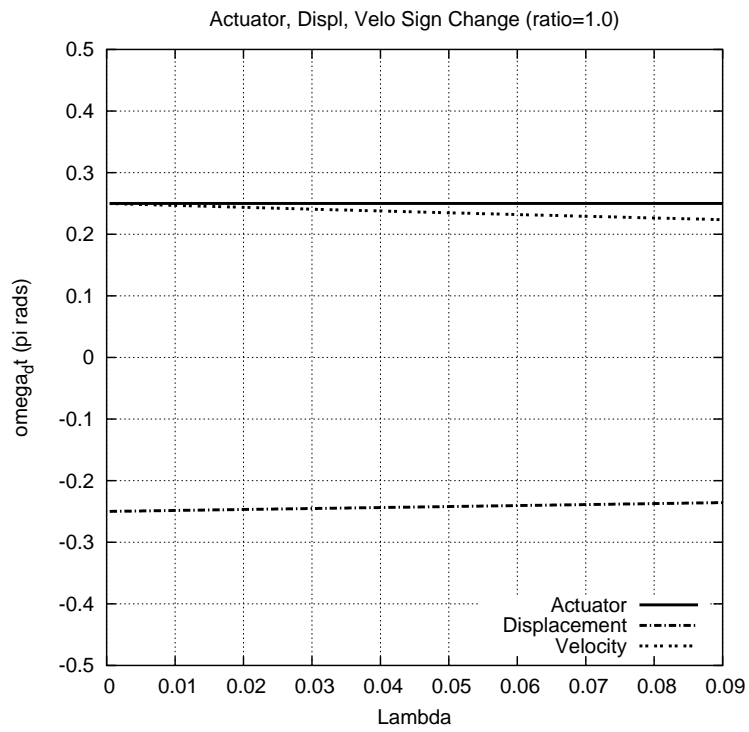
Figure 2.5: Actuator, Displacement, and Velocity Sign Change During Free Vibration ($\rho = 1$)
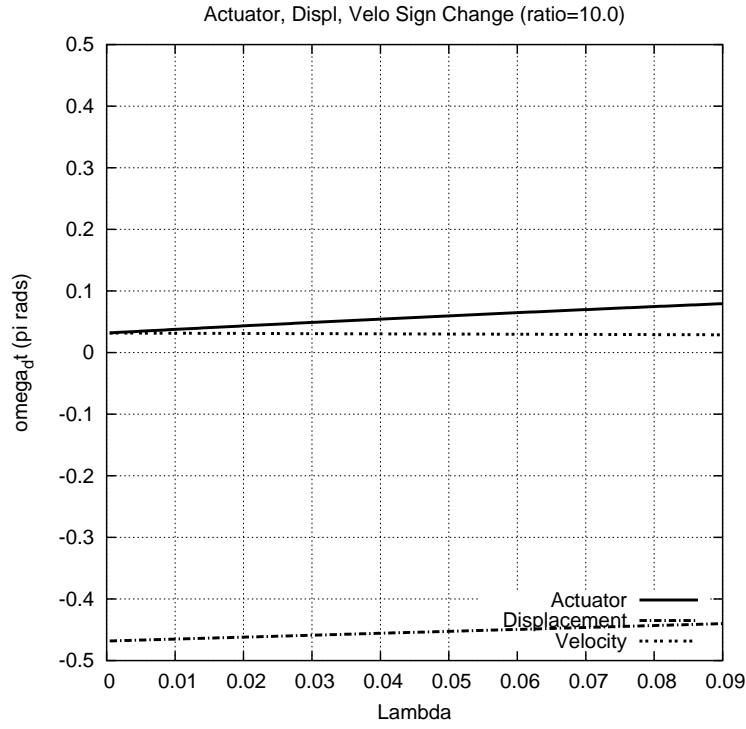
Figure 2.6: Actuator, Displacement, and Velocity Sign Change During Free Vibration ($\rho = 10$)

and

$$D = \frac{\dot{x}(0)}{2} + \frac{x(0)\xi w_o}{2w_o\sqrt{1-\xi^2}} - \frac{1}{4\xi w_o\sqrt{1-\xi^2}}\left(\xi\dot{x}(0) + (\xi + \sqrt{1-\xi^2})w_o x(0)\right). \tag{2.42}$$

Zero Displacements. The system displacements will change sign when,

$$\tan(w_d t) = \frac{-\sqrt{1-\xi^2}x(0)w_o}{\dot{x}(0) + x(0)w_o\xi}. \tag{2.43}$$

Zero Velocities. The system velocities will be zero when,

$$\tan(w_d t) = \frac{\dot{x}(0)\sqrt{1-\xi^2}}{\xi\dot{x}(0) + (\xi + \sqrt{1-\xi^2})w_o x(0)}. \tag{2.44}$$

Plots of "Phase of Bang-Bang Control" vs ξ.

Because the number of degrees of freedom in the model of free vibration response is one fewer than the corresponding steady state model (i.e., β is a constant value), one plot can display a complete picture of how the direction of control force application changes as a function of the remaining problem parameters. We simplify the problem by defining the dimensionless ratio,

21

$$\rho = \frac{x(0)w_o}{\dot{x}(0)}. \qquad (2.45)$$

Figures 2.4 through 2.6 are generated by solving equation 2.45 for $x(0)w_o$ and substituting into equations 2.39, 2.43, and 2.44 gives when the actuator, displacement and velocity of the system are zero in terms of ρ and ξ.

During the free vibration reponse, switching of the actuator force direction occurs almost in phase with the sign of velocity. This indicates that like the damping model, active control works to oppose changes in system displacement. Moreover, again notice that the displacement and velocity phase shifts are separated by $\pi/2$ radians. The "steady state" and "'free vibration" phase shift models are consistent if latter is viewed as a "steady state response" resulting from a very high forcing frequency (i.e., $\beta = g/w \to \infty$).

2.3 Research Avenue 2. Symbolic Analysis of Multi-Degree-of-Freedom Systems

2.3.1 Symbolic Representation for 2-DOF Bang-Bang Control Strategy

In this section we develop symbolic representation for the 2-DOF bang-bang control strategy under three objectives: (1) Minimization of potential energy, (2) Minimization of kinetic energy, and (3) Minimization of total (potential+kinetic) energy. We will soon see that "general symbolic expressions" are huge (even for a two degree of freedom structure) and computationally intactable (even for Mathematica$^{©}$) for large problems.

Minimizing Potential Energy

Recent research [9] suggests that overall "blanket minimization" of structure-level energy (i.e., potential and kenetic energy) is an overly simplified view of desirable behavior. Instead, analysis procedures should allow for potential energy terms in the system superstructure to be considered separately from potential energy in the base isolation devices. For the 2-DOF mass-spring-damper system shown in Figure 1.1, a suitable form for $\mathbf{Q}$ is:

$$\mathbf{Q} = \begin{bmatrix} a\gamma k + bk & -bk & 0 & 0 \\ -bk & bk & 0 & 0 \\ 0 & 0 & 0 & 0 \\ 0 & 0 & 0 & 0 \end{bmatrix}. \tag{2.46}$$

The parameter setting ($a = 1, b = 0$) corresponds to minimization of potential energy in the isolation device alone. Conversely, the parameter setting ($a = 0, b = 1$) corresponds to minimization of potential energy in the superstructure alone. The analysis assumes linear viscous damping of the form $\mathbf{C} = \alpha \cdot \mathbf{M} + \beta \cdot \mathbf{K}$ and that actuators may be located at either or both DOFs (weight on minimizing the potential energy in the first and second stories may be different).

Symbolic Solution. The symbolic solution to $\mathbf{A}^{\mathbf{T}}\mathbf{S} + \mathbf{S}\mathbf{A} = -\mathbf{Q}$ takes the form:

$$\mathbf{B}^{\mathbf{T}}\mathbf{S}(\mathbf{H}, m, k, \alpha, \beta, \gamma, a, b) = \mathbf{H}^{\mathbf{T}} \begin{bmatrix} \dfrac{f_{11}}{\text{Den 1}} & \dfrac{f_{12}}{\text{Den 1}} & \dfrac{f_{13}}{\text{Den 2}} & \dfrac{f_{14}}{\text{Den 2}} \\ \dfrac{f_{21}}{\text{Den 1}} & \dfrac{f_{22}}{\text{Den 1}} & \dfrac{f_{23}}{\text{Den 2}} & \dfrac{f_{24}}{\text{Den 2}} \end{bmatrix}. \tag{2.47}$$

Terms in the denominator are:

$$\text{Den 1} \;=\; 2(2\beta^2\gamma(2 + \gamma)k^2 + \alpha\beta(4 + 8\gamma + \gamma^2)km + m((4 + \gamma^2)k + 2\alpha^2(2 + \gamma)m)),$$

$$\text{Den 2} \;=\; 2(\beta^2\gamma k^2 + \alpha\beta(2+\gamma)km + \alpha^2 m^2)(2\beta^2\gamma(2+\gamma)k^2 + \alpha\beta(4+8\gamma+\gamma^2)km$$
$$+\, m((4+\gamma^2)k + 2\alpha^2(2+\gamma)m)).$$

And terms in the numerator are:

$$
\begin{aligned}
f_{11} \;=\;& bm((1+\alpha\beta)(2+\gamma)k + 2\alpha^2 m) + a(2\beta^2\gamma(2+\gamma)k^2 \\
& +\, \alpha\beta(2+7\gamma+\gamma^2)km + m((2-\gamma+\gamma^2)k + 2\alpha^2(1+\gamma)m)), \\[4pt]
f_{12} \;=\;& (a-b)m((1+\alpha\beta)(2+\gamma)k + 2\alpha^2 m) \\
\;=\;& -bm((1+\alpha\beta)(2+\gamma)k + 2\alpha^2 m) + am((1+\alpha\beta)(2+\gamma)k + 2\alpha^2 m), \\[4pt]
f_{13} \;=\;& m(bm(\alpha m((2+\gamma)k + 2\alpha^2 m) + \beta k(2\gamma k + 2\alpha^2 m + \alpha^2\gamma m)) \\
& +\, a(2\beta^3\gamma(2+\gamma)k^3 + \alpha\beta^2(4+12\gamma+3\gamma^2)k^2 m + \alpha m^2((2-\gamma+\gamma^2)k \\
& +\, 2\alpha^2(1+\gamma)m) + \beta km((4-2\gamma+\gamma^2)k + \alpha^2(6+9\gamma+\gamma^2)m)))), \\[4pt]
f_{14} \;=\;& m(-bm(-\beta\gamma^2 k^2 + \alpha^2\beta(2+3\gamma)km + 2\alpha^3 m^2 \\
& +\, \alpha k(\beta^2\gamma(2+\gamma)k - (-2+\gamma)m)) + a(2\beta^3\gamma(2+\gamma)k^3 \\
& +\, 2\alpha\beta^2(2+5\gamma+\gamma^2)k^2 m + \alpha m^2(-(-2+\gamma)k + 2\alpha^2 m) \\
& +\, \beta km(4k + \alpha^2(6+5\gamma)m)))), \\[4pt]
f_{21} \;=\;& (a-b)(2\beta^2\gamma(2+\gamma)k^2 + \alpha\beta(2+5\gamma)km + m((2-3\gamma)k + 2\alpha^2 m)) \\
\;=\;& -b(2\beta^2\gamma(2+\gamma)k^2 + \alpha\beta(2+5\gamma)km + m((2-3\gamma)k + 2\alpha^2 m)) \\
& +\, a(2\beta^2\gamma(2+\gamma)k^2 + \alpha\beta(2+5\gamma)km + m((2-3\gamma)k + 2\alpha^2 m)), \\[4pt]
f_{22} \;=\;& am((1+\alpha\beta)(2+\gamma)k + 2\alpha^2 m) + b(2\beta^2\gamma(2+\gamma)k^2 + \alpha\beta(2+7\gamma+\gamma^2)km \\
& +\, m((2-\gamma+\gamma^2)k + 2\alpha^2(1+\gamma)m)), \\[4pt]
f_{23} \;=\;& f_{14}, \\[4pt]
f_{24} \;=\;& m(b(2\beta^3\gamma^2(2+\gamma)k^3 + \alpha\beta^2\gamma(8+10\gamma+\gamma^2)k^2 m + \beta km(2\gamma k + \gamma^3 k + 2\alpha^2 m \\
& +\, 11\alpha^2\gamma m + 3\alpha^2\gamma^2 m) + \alpha m^2((2-\gamma+\gamma^2)k + 2\alpha^2(1+\gamma)m)) + a(2\beta^3\gamma(2+\gamma)k^3 \\
& +\, \alpha\beta^2(4+8\gamma+\gamma^2)k^2 m + \alpha m^2((2+\gamma)k + 2\alpha^2 m) + \beta km((4+2\gamma+\gamma^2)k + 3\alpha^2(2+\gamma)m))).
\end{aligned}
$$

Points to note are as follows:

1. This analysis demonstrates that symbolic representations for the $\mathbf{B}^{\mathsf{T}}\mathbf{S}$ matrix product are huge, even for a simple 2-dof system.

24

2. There are only two symbolic expressions for the denominators of $\mathbf{B^T S}$, one for the displacement coefficients, and a second for the velocity terms.

Special Cases

We have found that under a number of circumstances, the lengthy symbolic expressions simplify significantly.

Minimize Potential Energy ($k* = k$). When $\mathbf{Q}$ contains the structural stiffness matrix in the upper-left quadrant (i.e., $a = b = 1$), $\mathbf{B^T S}$ simplifies to:

$$\mathbf{B^T S} = \left[\begin{array}{cc} \frac{\mathbf{H^T}}{2} & \frac{\mathbf{H^T M}(\alpha \cdot \mathbf{M} + \beta \cdot \mathbf{K})^{-1}}{2} \end{array} \right].$$ (2.48)

This result is consistent with the n-DOF model derived in the next section.

Perfect Isolation ($\gamma = 0$). For structures that are perfectly isolated (i.e., $\gamma = 0$), the symbolic expressions simply to:

$$\mathbf{B^T S}(\mathbf{H}, m, k, \alpha, \beta, \gamma, a, b) = \mathbf{H^T} \left[\begin{array}{cccc} \frac{a+b}{4} & \frac{a-b}{4} & \frac{a(2\beta k+\alpha m)+b\alpha m}{4\alpha(2\beta k+\alpha m)} & \frac{a(2\beta k+\alpha m)-b\alpha m}{4\alpha(2\beta k+\alpha m)} \\ \frac{a-b}{4} & \frac{a+b}{4} & \frac{a(2\beta k+\alpha m)-b\alpha m}{4\alpha(2\beta k+\alpha m)} & \frac{a(2\beta k+\alpha m)+b\alpha m}{4\alpha(2\beta k+\alpha m)} \end{array} \right].$$ (2.49)

Two special cases exist. When $a = b = 1$, equation 2.49 simplifies further:

$$\mathbf{B^T S}(\mathbf{H}, m, k, \alpha, \beta, \gamma, 1, 1) = \mathbf{H^T} \left[\begin{array}{cccc} \frac{1}{2} & 0 & \frac{\beta k+\alpha m}{2\alpha(2\beta k+\alpha m)} & \frac{\beta k}{2\alpha(2\beta k+\alpha m)} \\ 0 & \frac{1}{2} & \frac{\beta k}{2\alpha(2\beta k+\alpha m)} & \frac{\beta k+\alpha m}{2\alpha(2\beta k+\alpha m)} \end{array} \right].$$ (2.50)

Notice that symbolic expressions for the coefficient denominators will be non-zero as long as $\alpha \neq 0$ (here we assume that m and k will never be zero) and hence, generally, the bang-bang control strategy is well defined even for structures that are perfectly isolated. The second special case occurs for $a = 0$ and $b = 1$ (i.e., we want to minimize energy within the superstructure alone). Now equation 2.49 simplifies to:

$$\mathbf{B^T S}(\mathbf{H}, m, k, \alpha, \beta, \gamma, 0, 1) = \mathbf{H^T} \left[\begin{array}{cccc} \frac{1}{4} & -\frac{1}{4} & \frac{\alpha m}{2\alpha(2\beta k+\alpha m)} & -\frac{\alpha m}{2\alpha(2\beta k+\alpha m)} \\ -\frac{1}{4} & \frac{1}{4} & -\frac{\alpha m}{2\alpha(2\beta k+\alpha m)} & \frac{\alpha m}{2\alpha(2\beta k+\alpha m)} \end{array} \right].$$ (2.51)

In a typical base isolated structure, the time history response will be dominated by the first mode of vibration (i.e., $x_1(t) \approx x_2(t)$ and $\dot{x}_1(t) \approx \dot{x}_2(t)$). We observe that displacement and velocity pairs of

25

this type will have little influence on the control strategy. Rather, it will be dominated by second-mode displacements.

Minimizing Kinetic Energy

This exercise can be repeated for minimization of kinetic energy in the base isolator and superstructure. For the 2-DOF mass-spring-damper system shown in Figure 1.1, a suitable form for $\mathbf{Q}$ is:

$$\mathbf{Q} = \begin{bmatrix} 0 & 0 & 0 & 0 \\ 0 & 0 & 0 & 0 \\ 0 & 0 & cm & 0 \\ 0 & 0 & 0 & dm \end{bmatrix}, \tag{2.52}$$

The symbols c and d in equation 2.52 represent relative amount of weight a designer places on minimizing kinetic energy in the first and second stories of the structure, respectively.

Appendix 1 contains a complete description of symbolic representations for the matrix elements in $\mathbf{B}^{\mathbf{T}}\mathbf{S}$. The elements of $\mathbf{B}^{\mathbf{T}}\mathbf{S}$ have rather long symbolic expressions, populated with the properties of the structure.

Minimizing Total (Potential+Kinetic) Energy

When $c = d = 1$, the symbolic representation of $\mathbf{B}^{\mathbf{T}}\mathbf{S}$ simplifies to:

$$\mathbf{B}^{\mathbf{T}}\mathbf{S} = \begin{bmatrix} \mathbf{0} & \frac{\mathbf{H}^{\mathbf{T}}\mathbf{M}(\alpha \cdot \mathbf{M} + \beta \cdot \mathbf{K})^{-1}}{2} \end{bmatrix}. \tag{2.53}$$

Notice that because solutions to the Lyapunov matrix equation are linear with respect to matrix S, the $\mathbf{B}^{\mathbf{T}}\mathbf{S}$ matrix product that minimizes the total (potential + kinetic) is simply the sum of equations 2.48 and 2.53.

2.3.2 Limitations of Symbolic Analysis with Mathematica©.

We attempted to compute symbolic expressions for systems having more than two degrees of freedom, but Mathematica's© demands for storage space are greater than what is available on standard workstations. Instead of returning symbolic expressions, the Mathematica© calculation either "times out" or aborts.

2.3.3 Symbolic Analysis of a N-DOF System

When we first obtained symbolic expressions for the matrix elements in $\mathbf{B}^{\mathbf{T}}\mathbf{S}$, it was not immediately evident that when $a = b = 1$ and $c = d$, the lengthy formulae would simplify to the formats shown in equations 2.48 and 2.53. This surprising result made us think about other possibilties. Specifically, "starting with relatively simple expressions for solutions to $\mathbf{B}^{\mathbf{T}}\mathbf{S}$ in a one degree of freedom structure, we wondered if it would it be possible – perhaps under certain restrictions – to scale this solution up to a N-DOF system?" This pathway of investigation has two key benefits. Unlike numerical procedures for solution to the Lyapunov equation, symbolic expressions provide physical insight into the inner workings of the bang-bang control strategy. And second, when the matrix restrictions apply, symbolic expressions remove the need for nontrivial numerical solutions to the Lyapunov matrix equation.

For a detailed explanation of restrictions that must exist on $\mathbf{M}$ and $\mathbf{K}$ in order for scalability to occur, the intersted reader is referred to Appendix 2. We now present a summary of the key results and observations.

Minimizing Potential Energy

To minimize the potential energy in a n-DOF system, an appropriate choice for the $\mathbf{Q}$ matrix would be:

$$\mathbf{Q} = \begin{bmatrix} \mathbf{K} & \mathbf{0} \\ \mathbf{0} & \mathbf{0} \end{bmatrix} ; \tag{2.54}$$

where $\mathbf{K}$ is the n x n structural stiffness matrix and $\mathbf{0}$ is a n x n matrix of zeros. Substituting equation 2.54 into the Lyapunov matrix equation shown in equation 1.11 and solving results in the following $\mathbf{B}^{\mathbf{T}}\mathbf{S}$ matrix product:

$$\mathbf{B}^{\mathbf{T}}\mathbf{S} = \begin{bmatrix} \frac{\mathbf{H}^{\mathbf{T}}}{2} & \frac{\mathbf{H}^{\mathbf{T}}\mathbf{M}(\alpha\cdot\mathbf{M}+\beta\cdot\mathbf{K})^{-1}}{2} \end{bmatrix} ; \tag{2.55}$$

where $\mathbf{H}$ is a n by p matrix that designates the location of the controller(s). Appendix 2 shows the derivation of equation 2.55.

Requirements for Scalability. Equation 2.55 holds when: (1) the mass matrix $\mathbf{M}$ is diagonal and uniform (i.e., $m_1 = m_2 = ... = m_n$), (2) linear viscous damping is present, and (3) the structural stiffness matrix $\mathbf{K}$ is well-conditioned. If the damping matrix sum $\alpha \cdot \mathbf{M} + \beta \cdot \mathbf{K}$ becomes rank deficient, then a unique solution to $\mathbf{B}^{\mathbf{T}}\mathbf{S}$ does not exist.

Remark. By substituting equation 2.55 into equation 1.12, the system parameters that are being minimized by the modified bang-bang control objective results:

$$\dot{V}[x(t), \dot{x}(t)] = -x^T(t)\mathbf{K}x(t) + u^T(t)\mathbf{H^T}[\mathbf{I}x(t) + \mathbf{M}(\alpha \cdot \mathbf{M} + \beta \cdot \mathbf{K})^{-1}\dot{x}(t)]. \tag{2.56}$$

The first term on the right-hand side of equation 2.56 is an energy term that correspondings to double the amount of potential energy in the system at any time, t. Physical considerations dictate that the second term on the right-hand side of equation 2.56 must also be in terms of energy. Since the actuator force, $u(t)$, is present in equation 2.56, this term may be thought of as being made up of displacement and velocity terms that account for work that is done by the actuator force(s) at any time, t.

Minimizing Kinetic Energy

The kinetic energy of a mass-spring system, $T(t)$, may be represented by the following equation:

$$T(\dot{x}(t)) = \frac{m_1 \dot{x}_1(t)^2}{2} + \frac{m_2 \dot{x}_2(t)^2}{2} + ... + \frac{m_n \dot{x}_n(t)^2}{2}. \tag{2.57}$$

Minimizing the squares of the velocities of a system response may not seem like an important parameter, but internal non-structural damage (e.g., to internal walls, plumbing, etc.) is correlated to peak velocities within a structure [31]. Accordingly, an appropriate choice for $\mathbf{Q}$ is as follows:

$$\mathbf{Q} = \begin{bmatrix} \mathbf{0} & \mathbf{0} \\ \mathbf{0} & \mathbf{M} \end{bmatrix}; \tag{2.58}$$

where $\mathbf{M}$ is the n by n structural mass matrix and $\mathbf{0}$ is a n by n matrix of zeros. Substituting equation 2.58 into the Lyapunov matrix equation results in the $\mathbf{B^T S}$ matrix product:

$$\mathbf{B^T S} = \begin{bmatrix} \mathbf{0} & \frac{\mathbf{H^T M}(\alpha \cdot \mathbf{M} + \beta \cdot \mathbf{K})^{-1}}{2} \end{bmatrix}. \tag{2.59}$$

In equation 2.59, $\mathbf{0}$ is a p by n matrix of zeros and $\mathbf{H}$ is a n by p matrix that designates the location of the controller(s). Appendix 2 shows the derivation of equation 2.59.

Requirements for Scalability. Equation 2.59 has the same scaleability requirements as equation 2.55.

Remark. By substituting equation 2.59 into equation 1.12 the system parameters that are being minimized by the modified bang-bang control objective results:

$$\dot{V}[\dot{x}(t)] = -\dot{x}^T(t)\mathbf{M}\dot{x}(t) + u^T(t)\mathbf{H^T}[\mathbf{M}(\alpha \cdot \mathbf{M} + \beta \cdot \mathbf{K})^{-1}\dot{x}(t)]. \tag{2.60}$$

In a manner analoguous to the case for minimizing the potential energy in a n-DOF system, the first term on the right-hand side of equation 2.60 is an energy term corresponding to double the amount of kinetic energy in the system at any time, t. Since the actuator force, $u(t)$, is present in the second term on the right-hand side of equation 2.60, this term may be thought of as being made up of only velocity terms that account for work that is done by the actuator force(s) at any time, t. It is noteworthy that by choosing the $\mathbf{Q}$ matrix as shown in equation 2.58, the modified bang-bang control objective works toward minimizing system velocities, and not system displacements.

Minimizing Total (Potential+Kinetic) Energy

The total energy in an n-DOF system can be minimized by setting $\mathbf{Q}$ to:

$$\mathbf{Q} = \left[\begin{array}{cc} \mathbf{K} & \mathbf{0} \\ \mathbf{0} & \mathbf{M} \end{array} \right]. \tag{2.61}$$

Solutions to the Lyapunov equation corresponding to equation 2.61 are given by the sum of equations 2.54 and 2.58. In other words,

$$\mathbf{B^T S} = \left[\begin{array}{cc} \frac{\mathbf{H^T}}{2} & \frac{\mathbf{H^T M}(\alpha \cdot \mathbf{M} + \beta \cdot \mathbf{K})^{-1}}{2} \end{array} \right] + \left[\begin{array}{cc} \mathbf{0} & \frac{\mathbf{H^T M}(\alpha \cdot \mathbf{M} + \beta \cdot \mathbf{K})^{-1}}{2} \end{array} \right] = \left[\begin{array}{cc} \frac{\mathbf{H^T}}{2} & \mathbf{H^T M}(\alpha \cdot \mathbf{M} + \beta \cdot \mathbf{K})^{-1} \end{array} \right].$$
$$\tag{2.62}$$

Remark. Substituting equation 2.62 into 1.12 gives the following equation:

$$\dot{V}[x(t), \dot{x}(t)] = -[x^T(t)\mathbf{K}x(t) + \dot{x}^T(t)\mathbf{M}\dot{x}(t)] + u^T(t)\mathbf{H^T}[\mathbf{I}x(t) + 2\mathbf{M}(\alpha \cdot \mathbf{M} + \beta \cdot \mathbf{K})^{-1}\dot{x}(t)]. \tag{2.63}$$

It is clear that equation 2.63 is equal to the sum of equations 2.56 and 2.60. The first and second terms on the right-hand side of equation 2.63 are energy terms corresponding to double the sum of potential and kinetic energy in the system at any time, t. The third term on the right-hand side of equation 2.63 may be thought of as being made up of displacement and velocity terms that account for work that is done by the actuator force(s) at any time, t.

2.4 Research Avenue 3. Sensitivity of Bang-Bang Control to Nonlinear Deformations

In this section we explore the sensitivity of parameters in modified bang-bang control to localized nonlinear deformations in the base isolation devices. A key observation is that in a typical base isolated structure, the initial stiffness of the base isolators will be 10-20% of the stiffness of elements in the superstructure. After the isolators have yielded, the tangent stiffness may drop to 2-10% of elements in the superstructure. From a research perspective, the question of interest is "do these nonlinearities have a significant impact on the control strategy that should be employed?" We address this concern by conducting a symbolic analysis of the control strategy for minimization of potential energy; see equation 2.55.

2.4.1 Case Study Problem (2-DOF Mass-Spring System)

The case study problem is the 2-DOF system shown in Figure 1.1. When controllers act on both degrees of freedom, $\mathbf{H}$ is as follows:

$$\mathbf{H} = \begin{bmatrix} 1 & 0 \\ 0 & 1 \end{bmatrix}.$$

(2.64)

Substituting equation 2.64 into equation 2.55 gives:

$$\mathbf{B^T S} = \begin{bmatrix} \frac{1}{2} & 0 & B^T S(1,3) & B^T S(1,4) \\ 0 & \frac{1}{2} & B^T S(2,3) & B^T S(2,4) \end{bmatrix} = \begin{bmatrix} \frac{\mathbf{H^T}}{2} & \frac{\mathbf{H^T M}(\alpha \cdot \mathbf{M} + \beta \cdot \mathbf{K})^{-1}}{2} \end{bmatrix}.$$

(2.65)

In the bang-bang control strategy, coefficients on the left- and right-hand sides of $\mathbf{B^T S}$ are multiplied by the system displacements and velocities, respectively. The terms $B^T S(1,3)$ through $B^T S(2,4)$ are elements of the matrix product $\frac{\mathbf{H^T M}(\alpha \cdot \mathbf{M} + \beta \cdot \mathbf{K})^{-1}}{2}$. Due to symmetry of the mass and stiffness matrices, $B^T S(2,3) = B^T S(1,4)$.

Our research goal is to identify conditions in the problem formulation where coefficients for the system velocities will be either very large or, conversely, very small, compared to the displacement coefficients. The former condition will lead to control strategies heavily influenced by system velocities. The latter will lead to control strategies dominated by system displacements.

2.4.2 Symbolic Expressions for Velocity Components of Bang-Bang Control

Let us assume that linear viscous damping is present in the form $\alpha \cdot \mathbf{M} + \beta \cdot \mathbf{K}$ such that there is percentage, ξ, of critical damping of the first two modes of vibration. Since detailed information on the variation of damping with frequency is seldom available, it is common practice for analysis procedures to assume equal damping ratios to both frequencies [18] (i.e., $\xi = \xi_1 \approx \xi_2$ where ξ_1 and ξ_2 respresent the damping ratios for the first two modes of vibration, respectively). The damping matrix coefficients α and β are as follows:

$$\alpha = \frac{2\xi\omega_2\omega_1}{\omega_2 + \omega_1}, \tag{2.66}$$

and

$$\beta = \frac{2\xi}{\omega_2 + \omega_1}, \tag{2.67}$$

where ω_1 and ω_2 are the first and second natural frequencies of the system, respectively. From eigenvalue analysis, the natural circular frequencies of vibration are:

$$\omega_1(\gamma, m, k) = \sqrt{\frac{k(\gamma + 2 - \sqrt{\gamma^2 + 4})}{2m}}, \tag{2.68}$$

and

$$\omega_2(\gamma, m, k) = \sqrt{\frac{k(\gamma + 2 + \sqrt{\gamma^2 + 4})}{2m}}. \tag{2.69}$$

Symbolic expressions for $B^T S(1,3)$, $B^T S(1,4)$ and $B^T S(2,4)$ in terms of ξ, γ, and the simplifying notation $\tau = m/k$ (units of seconds^2) are obtained in three steps. First, equations 2.68 and 2.69 are substituted into 2.66 and 2.67. Equations 2.66 and 2.67 are then substituted into equation 2.65. Finally, we note that $\omega_1\omega_2\tau = \sqrt{\gamma}$. The latter observation provides a pathway for simplifying the symbolic expressions to the point where key trends in the "velocity coefficients" can be identified. The symbolic expressions are as follows:

$$B^T S(1,3) = \left[\frac{\sqrt{\tau/8}\left[\sqrt{(\gamma+2) - \sqrt{\gamma^2 + 4}} + \sqrt{(\gamma+2) + \sqrt{\gamma^2 + 4}}\right](1 + \sqrt{\gamma})}{\sqrt{\gamma} \cdot [4 + 2\gamma + 4\sqrt{\gamma}] \cdot \xi} \right] \tag{2.70}$$

$$B^T S(1,4) = \left[\frac{\sqrt{\tau/8}\left[\sqrt{(\gamma+2) - \sqrt{\gamma^2 + 4}} + \sqrt{(\gamma+2) + \sqrt{\gamma^2 + 4}}\right]}{\sqrt{\gamma} \cdot [4 + 2\gamma + 4\sqrt{\gamma}] \cdot \xi} \right] \tag{2.71}$$

$$B^T S(2,4) = \left[\frac{\sqrt{\tau/8} \left[\sqrt{(\gamma + 2) - \sqrt{\gamma^2 + 4}} + \sqrt{(\gamma + 2) + \sqrt{\gamma^2 + 4}} \right] (1 + \gamma + \sqrt{\gamma})}{\sqrt{\gamma} \cdot [4 + 2\gamma + 4\sqrt{\gamma}] \cdot \xi} \right] \quad (2.72)$$

Remark. We need to make sure that the parameter values τ and γ are selected in such way that the natural periods of vibration are representative of systems that occur in practice. The derivation is straightforward. From equations 2.68 and 2.69 we obtain:

$$T_1 = \frac{2\pi}{w_1} = 2\pi \sqrt{\frac{2\tau}{\left(\gamma + 2 - \sqrt{\gamma^2 + 4} \right)}}, \quad (2.73)$$

and

$$T_2 = \frac{2\pi}{w_2} = 2\pi \sqrt{\frac{2\tau}{\left(\gamma + 2 + \sqrt{\gamma^2 + 4} \right)}}. \quad (2.74)$$

Table 2.1 summarizes the first and second natural periods of vibration (i.e., T_1 and T_2) for γ natural periods of vibration for γ covering the interval [0.0001, 0.15] at various levels of τ.

$\tau = 0.0001$ (sec^2)	$\gamma = 0.001$	$\gamma = 0.005$	$\gamma = 0.01$	$\gamma = 0.05$	$\gamma = 0.10$	$\gamma = 0.15$
T_1 (sec)	2.8103	1.2574	0.8897	0.3999	0.2846	0.2338
T_2 (sec)	0.0444	0.0444	0.0444	0.0442	0.0439	0.0436
$\tau = 0.0010$ (sec^2)	$\gamma = 0.001$	$\gamma = 0.005$	$\gamma = 0.01$	$\gamma = 0.05$	$\gamma = 0.10$	$\gamma = 0.15$
T_1 (sec)	8.8869	3.9763	2.8134	1.2646	0.8999	0.7395
T_2 (sec)	0.1405	0.1404	0.1403	0.1396	0.1387	0.1378
$\tau = 0.010$ (sec^2)	$\gamma = 0.001$	$\gamma = 0.005$	$\gamma = 0.01$	$\gamma = 0.05$	$\gamma = 0.10$	$\gamma = 0.15$
T_1 (sec)	28.1028	12.5742	8.8969	3.9989	2.8457	2.3385
T_2 (sec)	0.4442	0.4440	0.4437	0.4415	0.4387	0.4359

Table 2.1: First and Second Natural Periods of Vibration (i.e. T_1 and T_2) versus τ and γ

Generally speaking, low values of τ (i.e., $\tau \leq 0.0001$ secs^2) correspond to systems having a stiff superstructure. High values of τ (i.e., $\tau \geq 0.01$ secs^2) correspond to systems having a flexible superstructure. During a nonlinear time-history response, instantanious values of γ vary accoding to elastic/plastic states of the systems. In contrast, values of τ remain constant. Hence, from an analysis

and design perspective, we need to explore sensitivity of parameters in the bang-bang control strategy to systematic variations in γ while holding τ constant.

2.4.3 Sensitivity Analysis

In an effort to understand the relative importance of displacement and velocity terms in the bang-bang control strategy, we employ a combination of mathematics and graphics to identify and validate trends in the "system velocity coefficients" versus ξ, γ and τ. First, notice that although each formula has many terms, the relationship among these coefficients is simple:

$$\frac{B^T S(1,3)}{B^T S(1,4)} = 1 + \sqrt{\gamma} \quad \text{and} \quad \frac{B^T S(2,4)}{B^T S(1,4)} = 1 + \gamma + \sqrt{\gamma}. \tag{2.75}$$

For large values of γ (e.g., $\gamma = 0.15$), the ratios $B^T S(1,3)/B^T S(1,4)$ and $B^T S(2,4)/B^T S(1,4)$ are 1.38 and 1.53, respectively. For small values of γ (i.e., $\gamma \sim 0.00$), the ratios $B^T S(1,3)/B^T S(1,4)$ and $B^T S(2,4)/B^T S(1,4)$ approach 1. Hence, while the left-hand side of $\mathbf{B^T S}$ has coefficient values 1/2 along the diagonal elements and zeros elsewhere, for small values of γ, values of the four system velocity components are approximately the same. Moreover, we note that:

$$\text{limit}_{\gamma \to 0} \left[\frac{\sqrt{(\gamma+2) - \sqrt{\gamma^2 + 4}} + \sqrt{(\gamma+2) + \sqrt{\gamma^2 + 4}}}{[4 + 2\gamma + 4\sqrt{\gamma}]} \right] = \frac{1}{2}. \tag{2.76}$$

Hence, for small values of γ, the velocity coefficients $B^T S(1,3)$, $B^T S(1,4)$ and $B^T S(2,4)$ increase in proportion to $1/\sqrt{\gamma}$. Also, for a fixed value of γ, the velocity coefficients increase in proportion to $\sqrt{\tau}$ and $1/\xi$ (the damping ratio of the structure).

Figures 2.7 through 2.9 validate these observations and show two important trends. First, we observe that τ increases monotonically as one moves vertically along contours of constant γ. We conclude from this trend that the influence of system velocities on bang-bang control will increase as the superstructure becomes progressively more flexible. (Conversely, bang-bang control will be most influenced by system displacements when the superstructure is stiff.) Second, within the interval $\gamma \in$ [0.05,0.15], the coefficient values are relatively constant. We surmise from this observation that "sub-optimal bang-bang control strategies" will be insensitive to localized nonlinearities in the base isolation devices, especially when $\gamma(t)$ remains within the interval [0.05,0.15]. As such, simplified design procedures might be justified. For design applications where post-yield stiffnesses are very low (i.e., $\min (\gamma(t)) \approx 0$), the bang-bang control strategy is likely to switch between two modes: (1) a displacement driven strategy
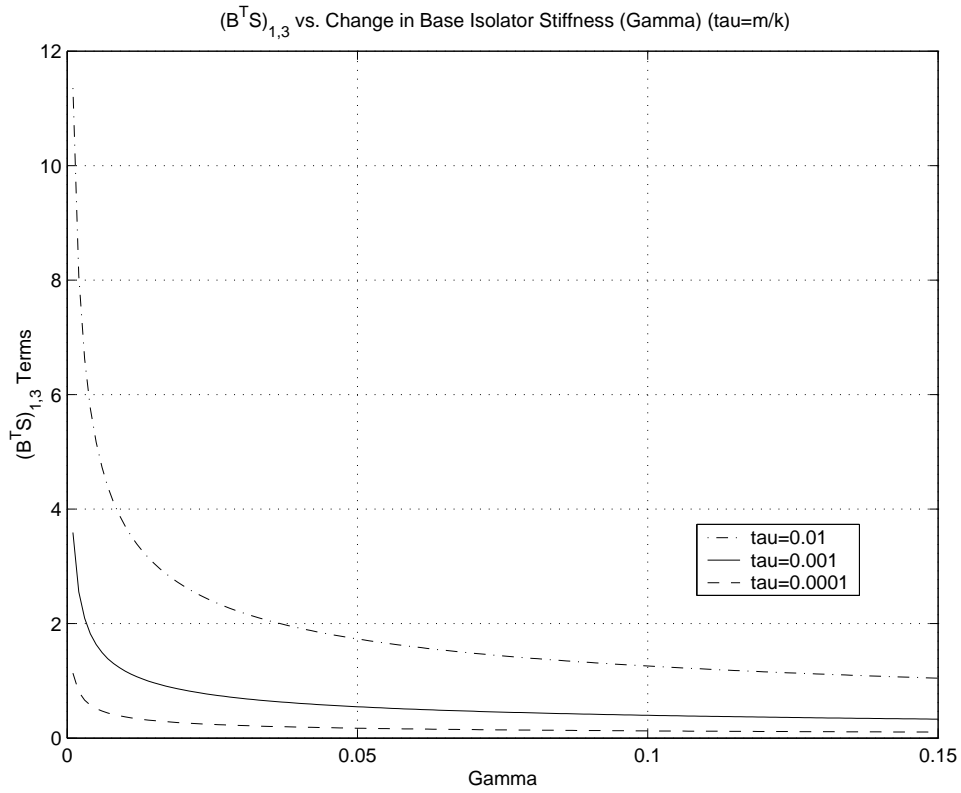
Figure 2.7: Velocity coefficient $B^T S(1,3)$ versus γ for contours of constant τ

for pre-yield states, and (2) a velocity driven strategy for post-yield states. At this point these observations are preliminary predictions. Numerical simulations are needed to validate the accuracy of these observations.

2.4.4 Consistency Check

At a glance this result would seem to be at odds with the symbolic expressions derived in Research Avenue 2. However, this isn't the case. Unlike the analysis in Section 2.3.1, the formulation here assumes that the damping matrix coefficients α and β, i.e.,

$$\alpha = \frac{2\xi\omega_2\omega_1}{\omega_2 + \omega_1} \qquad \text{and} \qquad \beta = \frac{2\xi}{\omega_2 + \omega_1}, \tag{2.77}$$

will vary according to ω_1 and ω_2, the first and second natural circular frequencies of the system, respectively. As γ approaches zero, the natural periods of vibration move toward infinity. Hence, it is evident from equation 2.77 that as ω_1 and ω_1 approach 0, β increases toward infinity. The case for α is less clear. We note that $w_1 < w_2$ (generally) and rewrite the symbolic expression for α as

34

$$\alpha = \frac{2\xi\omega_1}{\left[1 + \frac{\omega_1}{\omega_2}\right]}. \tag{2.78}$$

The denominator will evaluate to a small finite number as γ approaches zero. Hence, α also approaches 0. Moreoever, from equation 2.50 we see that as α approaches 0, coefficients $B^T S(1,3)$ and $B^T S(1,4)$ increase in value toward infinity. Coefficients $B^T S(1,3)$ and $B^T S(1,4)$ also approach each other in value. Therefore, these observations are completely consistent with the symbolic analysis in Section 2.2.

Remark. Although Rayleigh damping models are not associated with single degree-of-freedom systems, it can be easily shown that if $w_1 = w_2$ in equations 2.77, the damping coefficient

$$c = \left[\frac{1}{6\xi\omega}\right]. \tag{2.79}$$

Hence, even in the single degree-of-freedom case, the coupling of Rayleigh damping models to the bang-bang control strategy forces the damping coefficient to increase toward infinity as ω approaches zero.
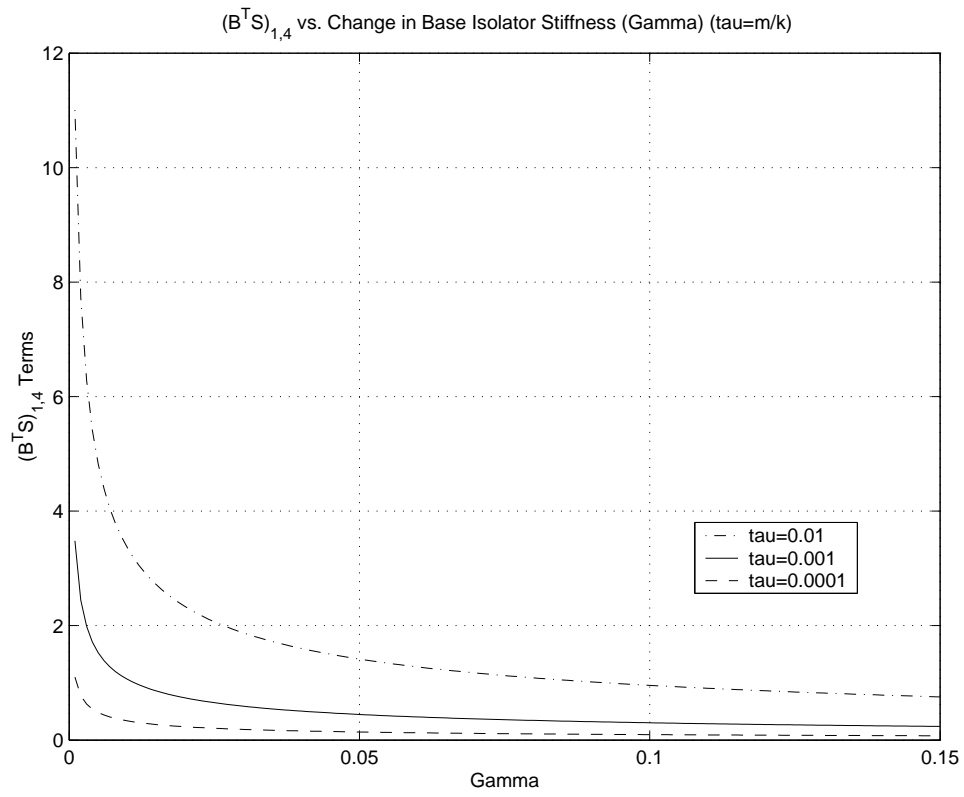
Figure 2.8: Velocity coefficient $B^T S(1,4)$ versus γ for contours of constant τ
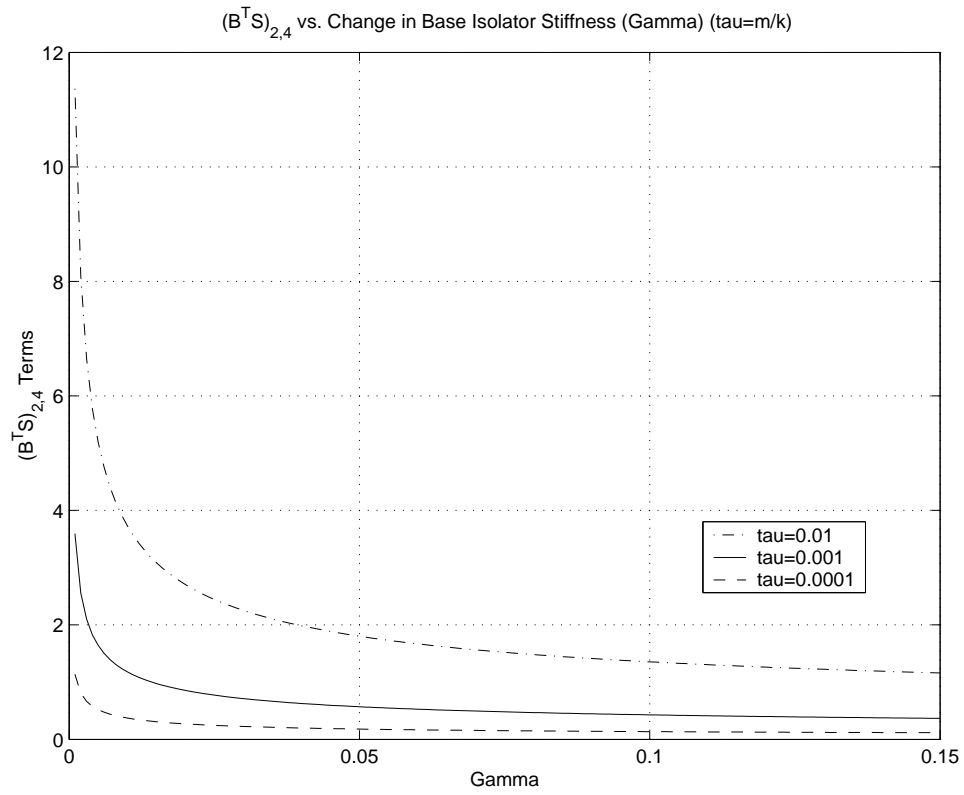
Figure 2.9: Velocity coefficient $B^T S(2,4)$ versus γ for contours of constant τ

36

Chapter 3

Numerical Experiments

For a wide range of moderate-to-large ground motion events, base isolated structures are expected to exhibit nonlinear displacement behavior at the isolator level, leaving the main structural system undamaged. In Section 2.4 we formulated symbolic expressions for parameters in the bang-bang control strategy as a function of localized nonlinear deformations in the isolator devices. Figures 2.7 through 2.9 indicate that over the interval $\gamma \in [0.05, 0.15]$, the magnitude of velocity coefficients in $\mathbf{B}^{\mathbf{T}}\mathbf{S}$ will be insensitive to variations in γ. From a design perspective, however, we need to know whether small variations in the magnitude of velocity coefficients will lead to large perturbations in peak values of system response? To resolve this issue, in this chapter we use the Aladdin scripting language [6, 7] to compute the time-history response of a five-DOF actively controlled nonlinear mass-spring-damper system subject to an ensemble of severe earthquake ground motions. The purposes of this experiment are to: (1) Validate by experiment the theoretical formulation for modified bang-bang control, (2) Demonstrate that the effectiveness of modified bang-bang control is insensitive to localized nonlinearities in the base isolation devices, and (3) Show the characteristic high frequency switching of the control force from one extreme to another after the ground excitation ends. The latter points to the limitations of constant applitude bang-bang control, and the strong need for a time-varying adaptive strategy.

3.1   Actively Controlled Mass-Spring-Damper System

Figures 3.1 and 3.2 show elevation views of an idealized mass-spring-damper base isolated system. Within the superstructure (elements 2-5), five lumped masses are connected via four linearly elastic springs. Element 1 is modeled with a bi-linear, force-displacement relationship that follows the kinematic hardening rule. Element 1 is used by Lin [27] and is a model of a laminated rubber base-isolator with a lead core. The purpose of element 1 is to isolate the superstructure from the inertia forces

DOF/Mode	Floor Mass (kg)	Stiffness (kN/m)		Period (secs)		Part. Factor (Γ)	
		Preyield	Postyield	Preyield	Postyield	Preyield	Postyield
1	160,000	27,000	4,500	1.20	2.70	1.11	1.02
2	160,000	150,000	150,000	0.31	0.33	0.15	0.03
3	160,000	150,000	150,000	0.17	0.17	0.04	0.01
4	160,000	150,000	150,000	0.13	0.13	0.02	0.00
5	160,000	150,000	150,000	0.11	0.11	0.01	0.00

Table 3.1: Properties of Five DOF Mass-Spring-Damper System

generated by the ground displacements. The left-hand side of Table 3.1 contains a summary of mass and stiffness properties for the structural model.

As shown on the right-hand side of Table 3.1, the first and second natural periods of vibration are 1.2 and 0.31 seconds, respectively. When the base isolator yields the first and second natural periods of vibration increase to 2.70 and 0.33 seconds. Also notice that in both the pre- and post-yield states, the modal participation factors indicate that the overall system response should be dominated by first mode displacements – this is particularly the case for post-yield displacements.

The yield force and displacement for element 1 are 350 kN and 13.0 mm, respectively. Damping effects are accounted for through linear viscous damping. In the equation $\mathbf{C} = \alpha\mathbf{M} + \beta\mathbf{K}$, the coefficients α and β are chosen so that there is 5% critical damping in the first two modes. Boundary conditions for our model are full-fixity at the base, and full-fixity against vertical displacements and rotations at nodes 2 through 5.

With respect to parameters in the symbolic analysis, the pre- and post-yield values of γ are 0.18 and 0.03 and the value for τ is 0.00106 secs^2. To see where these parameters lie with respect to the two-DOF system in Table 2.1, we partition the overall mass into two "roughly equivalent" masses. The ratio $\tau = 2.5m/k = 0.00265$ secs^2. These parameter settings: (1) put the pre-yield five-DOF between the bottom right-hand corner and middle right-hand side of Table 2.1, and (2) indicate that the study problem is consistent with the class of problems covered by the symbolic analysis.

3.2 Actuator Placement and Performance

For the purposes of illustrating the potential benefits of active control, an actuator is located at the top of the lead-rubber base isolator (degree of freedom 1). Unfortunately, at this time there is a complete lack of guidance in the literature on the selection of appropriate max/min forces in the actuator.
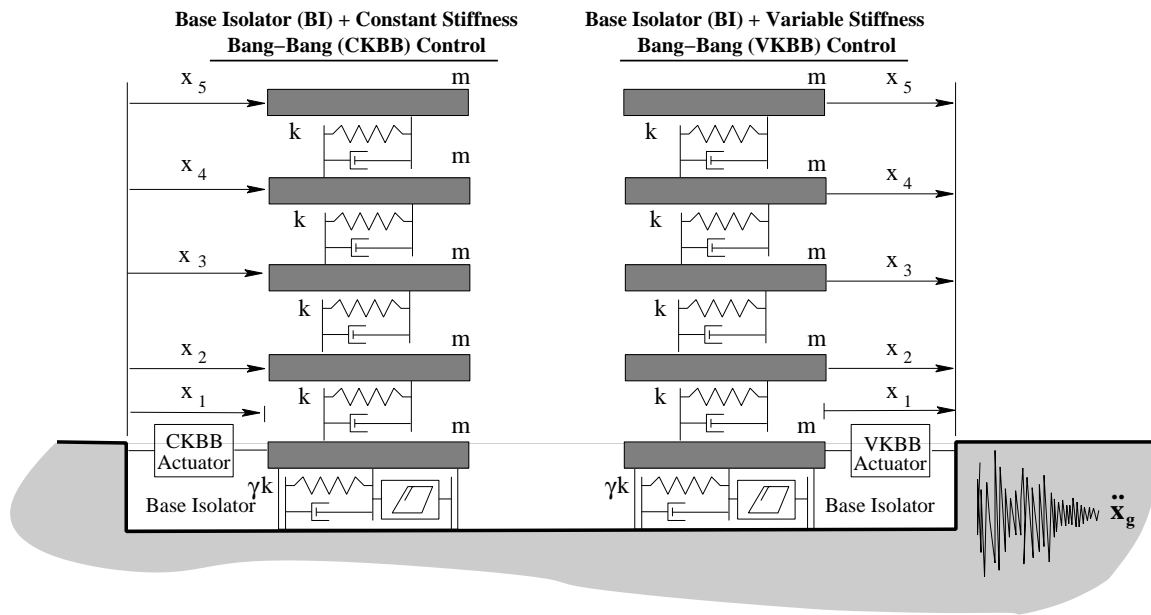
Figure 3.1: Elevation View of 5 DOF Linear/Nonlinear Mass-Spring-Damper System

Hence, in this study, we proceed under the assumption that the hybrid system will not add value to the overall system performance unless the passive and active components of control can work in concert. For the passive control system, stiffness and yield force design parameters are selected so that the structure will have appropriate natural periods of vibration and yield before excessive forces occur within the main structural system. We observe that since the actuators will not affect the natural periods of vibration, as a first cut, peak actuator forces should be balanced against the yield capacity of the isolators. Therefore, for this study, the maximum force that may be generated by the actuator matches the yield force of the base isolator (i.e., $u_{max} = 1 f_y = 350$ kN).

3.3   Ground Excitation

The numerical experiments are based on 15 second segments of ground motion recorded at San Fernando and Northridge, CA., Kobe, Japan, and Duzce, Turkey (Source, Earthquake Engineering Research (PEER) Center Strong Motion Database [21]). The details of each accelerogram are as follows:

1. 1971 San Fernando – 164° south-south-west component of the February 9, 1971, San Fernando, CA. USA. earthquake (unscaled magnitude 6.6). Recorded at the 279 Pacoima Dam substation (CDMG station #279). The closest distance of the substation to the fault rupture is 2.8 kilometers.

39
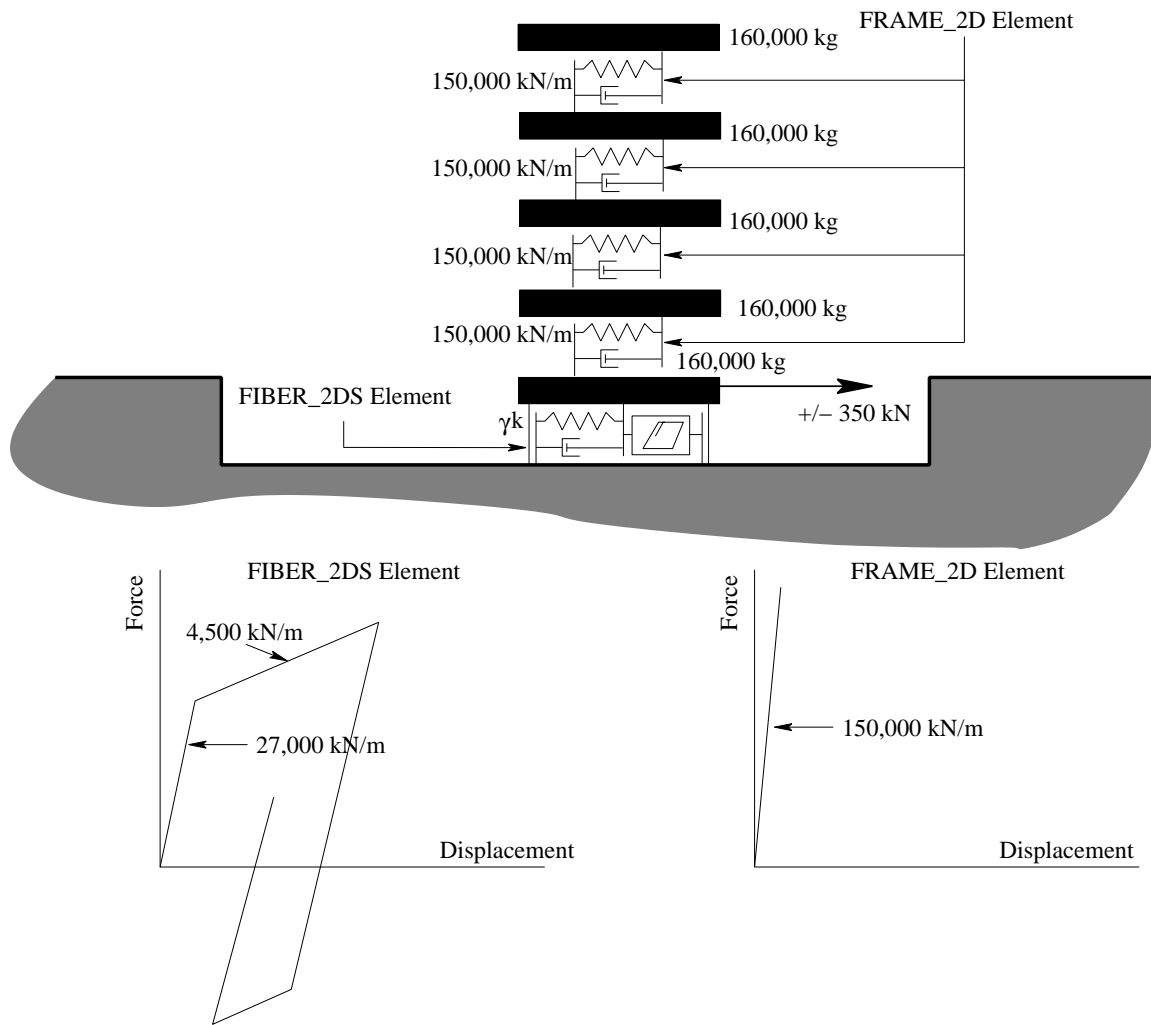
Figure 3.2: Model of Mass-Spring-Damper System

2. 1994 Northridge – east-west component of the January 17, 1994, Northridge, CA. USA. earthquake (unscaled magnitude 6.7). Recorded at the 24436 Tarzana, Cedar Hill substation (CDMG station 24436). The closest distance of the substation to the fault rupture is 17.5 kilometers.

3. 1995 Kobe – north-south component of the January 16, 1995, Kobe, Japan earthquake (unscaled magnitude 6.9). Recorded at the Kobe Japanese Meteorological Agency (KJMA). The closest distance of the substatation to the fault rupture is 0.6 kilometers.

4. 1999 Duzce – north-south component of the November 12, 1999, Duzce, Turkey earthquake (unscaled magnitude 7.1). Recorded at the 375 Lamont Doherty Earth Observatory substation. The closest distance of the substation to the fault rupture is 8.2 kilometers.

Earthquake	Motion Scale Factor	Arias Intensity (m/sec)	PGA (g)	Velocity (cm/sec)		Fourier Peak (secs)
				Min.	Max.	
1971 San Fernando	1.186	12.07	1.451	-30.69	181.30	0.21
1994 Northridge	0.779	12.07	1.388	-104.30	44.08	0.35
1995 Kobe	1.205	12.07	0.989	-100.30	90.27	0.68
1999 Duzce	1.131	12.07	1.073	-44.34	32.76	0.34

Table 3.2: Scaled Components of Ground Motion Excitations

Time histories of ground acceleration vs time are shown in Figures 3.3 through 3.6. The ground motions are digitized at intervals of 0.02 seconds. Each record was translated along the y-axis to remove residual velocity effects. Park and Otsuka [32] have classified these earthquakes as being severe – therefore, expected structural behavior is large plastic deformations in the isolators and essentially elastic behavior in the system superstructure.

Frequency Content of Ground Motions. The Fourier transform is a frequency domain analysis technique that is used to determine dominant frequency. Figures 3.7 through 3.10 show the frequency content of ground motion for the Kobe, San Fernando, Northridge and Duzce accelerograms, respectively. Each plot is annotated with the dominant frequency (Hz) and corresponding period (sec) of ground shaking (i.e., 0.20, 0.35, 0.68 and 0.34 seconds). It is important to note that in all cases, the base isolation design effectively separates the dominant period of vibration in the ground shaking from the natural periods of the structure ($T_1 = 1.2$ seconds). The corresponding values of $\beta = g/w$ are 6, 3.42, 1,47, and 3.52.

Ground Motion Scaling. Using peak ground acceleration (PGA) and Arias Intensity as metrics of ground shaking severity, the accelerograms were scaled so that they have approximately the same potential for imparting damage to a structure. Arias Intensity is a measure of energy in an accelerogram [4]. Kayen and Mitchell [26] note that as a scaling parameter, Arias Intensity has two key advantages over PGA, namely:

1. Arias Intensity is computed over the duration of the acceleration record. It therefore incorporates all amplitude cycles that occur. PGA, in contrast, utilizes a single amplitude that is independent of shaking duration, and

2. Arias intensity incorporates the severity of motions over the full range of recorded frequency, whereas, PGA is often associated only with high-frequency motion.

The scaling procedure constrains each ground motion to have equal Arias Intensity and adjusts the scaling factors so that the average peak ground acceleration has a desired level. Mathematically, if $\ddot{x}_{ig}(t)$ is the

41
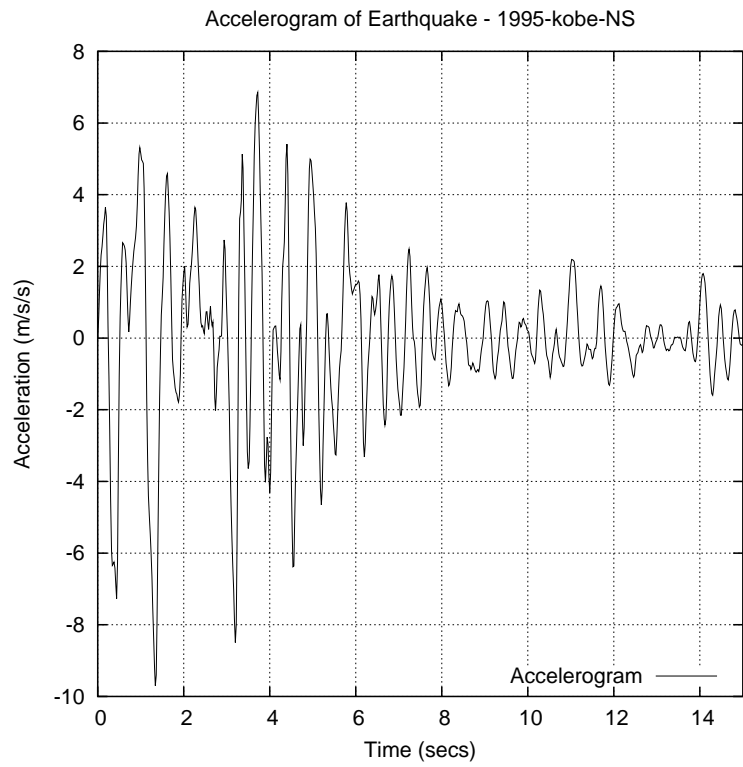
Figure 3.3: 1995 Kobe Accelerogram.
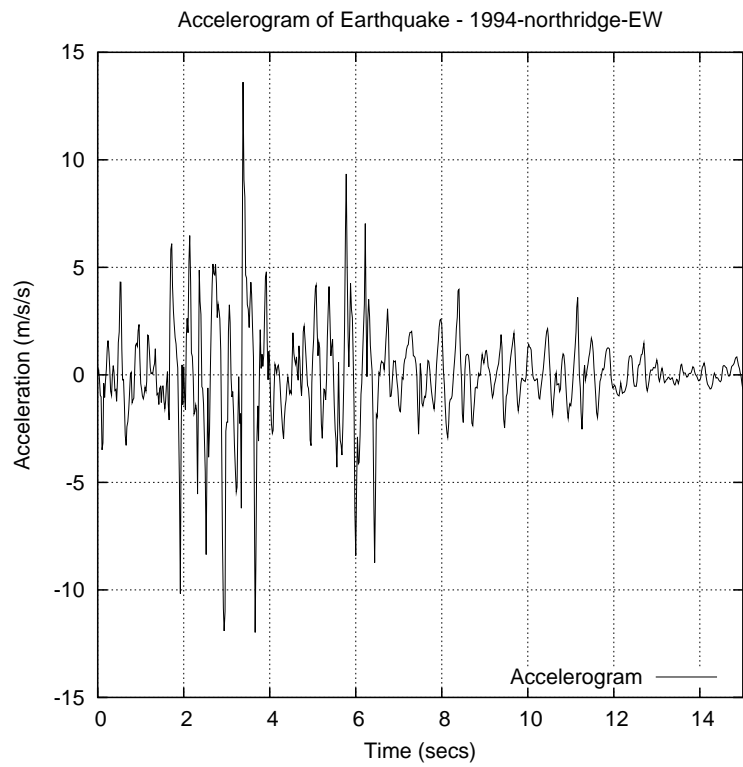
Figure 3.4: 1971 San Fernando Accelerogram.

42
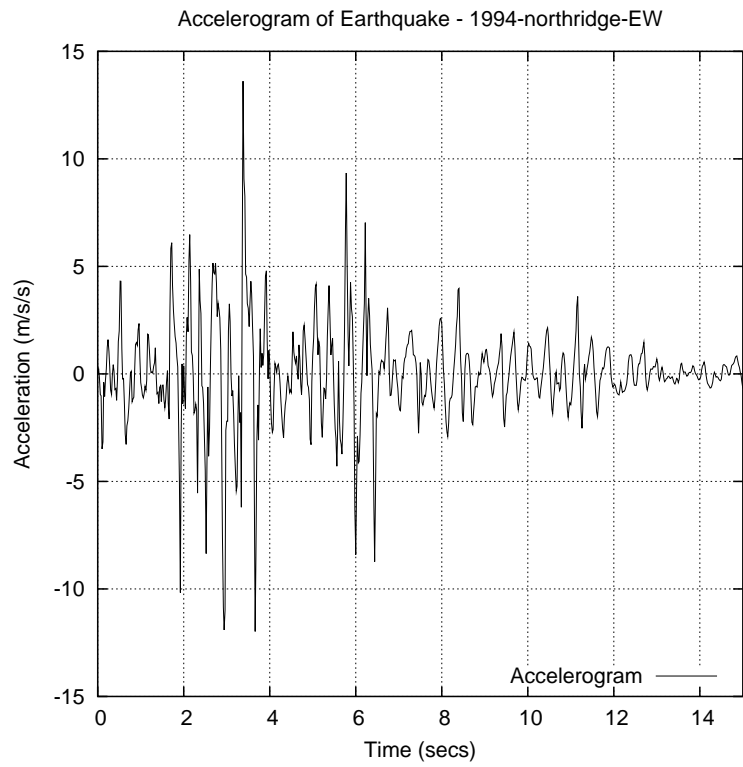
Figure 3.5: 1994 Northridge Accelerogram
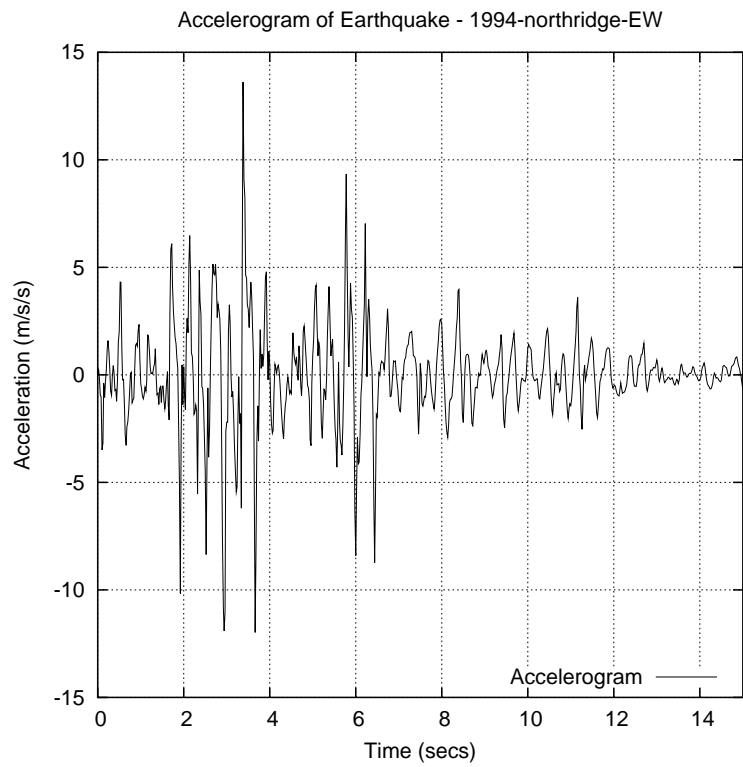
Figure 3.6: 1999 Duzce Accerogram.
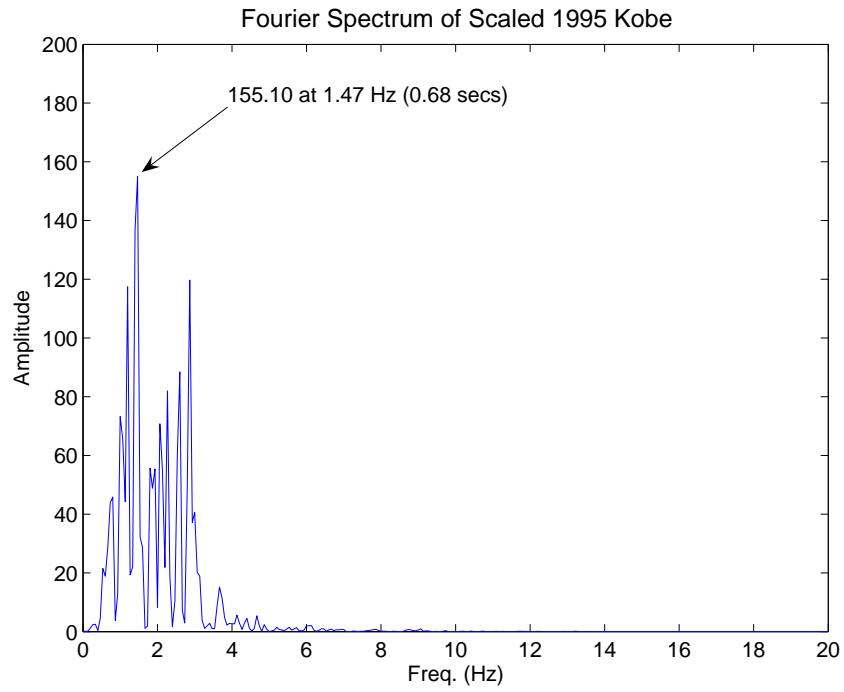
Figure 3.7: Fourier Spectrum for 1995 Kobe Accelerogram.
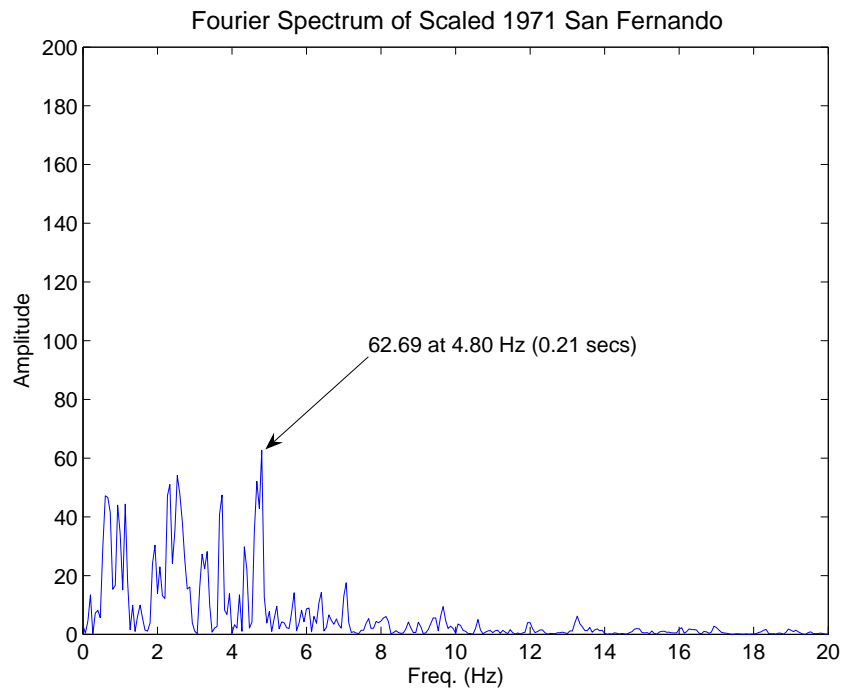
Figure 3.8: Fourier Spectrum for 1971 San Fernando Accelerogram.

44
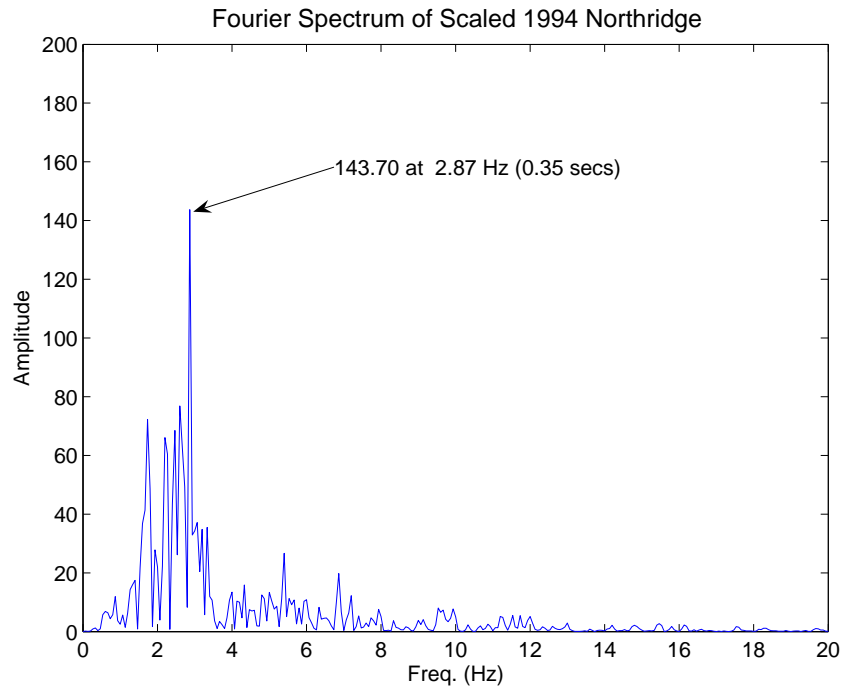
Figure 3.9: Fourier Spectrum for 1994 Northridge Accelerogram
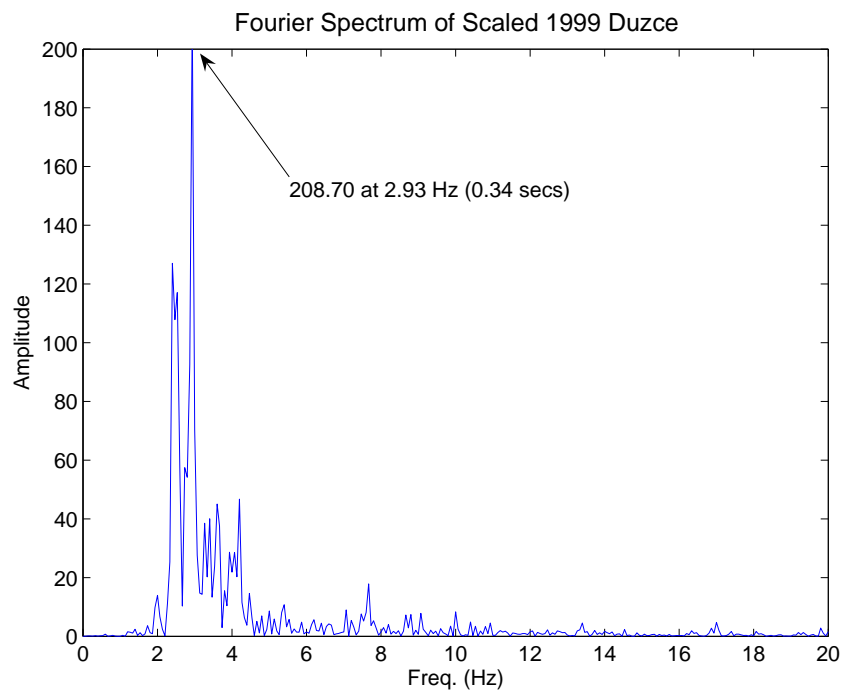
Figure 3.10: Fourier Spectrum for 1999 Duzce Accerogram.
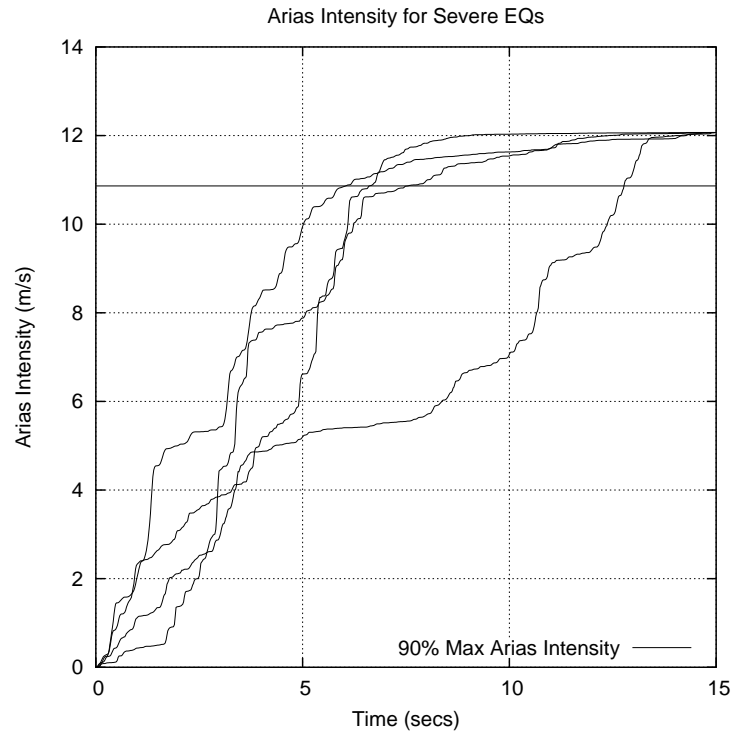
Figure 3.11: Arias Intensities versus Time for Scaled Ground Motion Accelerograms

i-th ground motion acceleration, then we seek scaling coefficients k_i so that:

$$\frac{\pi}{2g} \int_0^{10} k_1^2 \ddot{x}_{1g}^2(\tau)d\tau = \frac{\pi}{2g} \int_0^{10} k_2^2 \ddot{x}_{2g}^2(\tau)d\tau = \cdots = \frac{\pi}{2g} \int_0^{10} k_6^2 \ddot{x}_{6g}^2(\tau)d\tau = \text{constant}. \qquad (3.1)$$

The Arias Intensity and average PGA for the scaled ground motion accelerograms are 12.07 m/sec and 1.225g, respectively. Table 3.2 shows results of the scaling procedures, including the ground motion scaling factor, Arias Intensity, PGA, minimum and maximum ground velocities, and the period at which the peak Fourier transform occurs. The time variation in Arias Intensity for each of the four scaled ground motions is shown in Figure 3.11.

46

3.4   Impact of Control Algorithm Strategy on Nonlinear Behavior

The purpose of this section is to assess the impact of the control algorithm strategy on nonlinear system-level behavior; for details on underlying behavior, see equation 1.1. Time history analyses are computed for two control methodologies:

Control Methodology 1.   Consists of an actively controlled, nonlinear, base isolated mass-spring-damper system with the same section, material, and actuator properties as previously described. This simplified approach to control assumes that the structural system properties will remain constant throughout the analyses – but, of course, they don't. Prior to the commencement of time history computations, $\mathbf{B^T S}$ is calculated using values of α, β, $\mathbf{M}$, and $\mathbf{K}$ based on the elastic stiffness of the base isolator. Herein, this control methodology will be called constant stiffness (K) bang-bang (CKBB) control.

Control Methodology 2.   Consists of an actively controlled, nonlinear, base isolated mass-spring-damper system with the same section, material, and actuator properties as previously described. The goals of this methodology are to systematically refine the control algorithm based upon real-time values of the system parameters (including nonlinear force-displacement behavior of the isolation devices). A naive implementation would simply compute $\mathbf{B^T S}$ at each time-step. Instead, we note that at any point in time, the system can only be in one of two states: (1) pre-yield (initial) structural stiffness, or (2) post-yield (tangent) structural stiffness. $\mathbf{B^T S}$ was calculated prior to the time history using the base isolator stiffness based on both the preyield and postyield states. When the tangent stiffness of the base isolator is used to calculate $\mathbf{B^T S}$, equation 2.55 is not applicable. This is due to the fact that equation 2.55 was derived based on the relationship between the damping and stiffness (and mass) being $\mathbf{C} = \alpha \mathbf{M} + \beta \mathbf{K}$. However, since we are not varying the damping as a function of time, the Lyapunov equation (1.11) must be solved. During each time step of the analysis, an appropriate $\mathbf{B^T S}$ was selected. Herein, this control methodology will be called variable stiffness (K) bang-bang (VKBB) control.

To benchmark the improvements in system response due to the presence of active control, we compute a third time history response for base isolation alone. By comparing contours of time history response for control methodologies 1 and 2, we hope to determine if the simplifying assumptions in control methodology 1 are sufficient for design purposes. And by comparing control methodologies 1 and 2 to the ensemble of time history responses corresponding to base isolation alone, we hope to assess the impact

47

that active control can have as a supplement to base isolation.

3.4.1   Constant Stiffness Bang-Bang Control (CKBB)

Before linear modified bang-bang control can be applied to equation of motion, 1.1, $\mathbf{B}^{\mathbf{T}}\mathbf{S}$ must first be calculated. For both the control methodologies, the potential energy in the structure will be minimized (i.e., a = b = 1). Therefore, equation 3.2 is applicable:

$$\mathbf{B}^{\mathbf{T}}\mathbf{S} = \left[\begin{array}{cc} \frac{\mathbf{H}^{\mathbf{T}}}{2} & \frac{\mathbf{H}^{\mathbf{T}}\mathbf{M}(\alpha\cdot\mathbf{M}+\beta\cdot\mathbf{K})^{-1}}{2} \end{array} \right]. \tag{3.2}$$

Equation 3.2 evaluates to a (1×10) matrix.

Equations 3.3 through 3.5 show the values for α, β, and the matrices $\mathbf{H}$, $\mathbf{M}$, and $\mathbf{K}$ that are directly substituted into equation 3.2:

$$\alpha = 0.4170 \text{ Hz}; \quad \beta = 0.0039 \text{ secs}; \quad \mathbf{H} = \begin{bmatrix} 1 \\ 0 \\ 0 \\ 0 \\ 0 \end{bmatrix}, \tag{3.3}$$

$$\mathbf{M} = \begin{bmatrix} 177,000 & 0 & 0 & 0 & 0 \\ 0 & 160,000 & 0 & 0 & 0 \\ 0 & 0 & 160,000 & 0 & 0 \\ 0 & 0 & 0 & 160,000 & 0 \\ 0 & 0 & 0 & 0 & 160,000 \end{bmatrix} kg, \tag{3.4}$$

$$\mathbf{K} = \begin{bmatrix} 166,000 & -150,000 & 0 & 0 & 0 \\ -150,000 & 300,000 & -150,000 & 0 & 0 \\ 0 & -150,000 & 300,000 & -150,000 & 0 \\ 0 & 0 & -150,000 & 300,000 & -150,000 \\ 0 & 0 & 0 & -150,000 & 150,000 \end{bmatrix} kN/m, \tag{3.5}$$

and equation 3.6 shows the resultant matrix:

$$\mathbf{B}^{\mathbf{T}}\mathbf{S} = \left[\begin{array}{cccccccccc} 0.500 & 0 & 0 & 0 & 0 & 0.250s & 0.186s & 0.144s & 0.119s & 0.106s \end{array} \right]. \tag{3.6}$$

Matrix terms on the right-hand side of equation 3.6 are annotated with "s" indicating that the velocity terms have their own units.

48

3.4.2   Variable Stiffness Bang-Bang Control (VKBB)

For both control methodologies, the application of nonlinear modified bang-bang control is only slightly more difficult than linear modified bang-bang control. Since the only nonlinearity present in our numerical examples comes in the form of a bilinear base isolator stiffness, $\mathbf{B^TS}$ must be calculated exactly twice. Equation 3.7 shows the stiffness matrix, $\mathbf{K}$ that is directly substituted into equation 3.2. $\mathbf{H}$ and $\mathbf{M}$ are as shown in equations 3.3 and 3.4:

$$\mathbf{K} = \begin{bmatrix} 154,500 & -150,000 & 0 & 0 & 0 \\ -150,000 & 300,000 & -150,000 & 0 & 0 \\ 0 & -150,000 & 300,000 & -150,000 & 0 \\ 0 & 0 & -150,000 & 300,000 & -150,000 \\ 0 & 0 & 0 & -150,000 & 150,000 \end{bmatrix} kN/m. \qquad (3.7)$$

At each time step, the structural stiffness state must be determined and the corresponding $\mathbf{B^TS}$ substituted in the equation of motion. It is important to note, however, that when the post-yield tangent stiffness is employed in the $\mathbf{B^TS}$ computation, the relationship $\mathbf{C} = \alpha\mathbf{M} + \beta\mathbf{K}$ no longer holds, and hence, equation 2.55 is no longer valid. We circumvent this problem by computing a numerical solution to the Lyapanov equation. The result is:

$$\mathbf{B^TS} = \begin{bmatrix} 0.619 & -0.06 & -0.035 & -0.016 & -0.008 & 0.293s & 0.21s & 0.157s & 0.127s & 0.113s \end{bmatrix}.$$
$$(3.8)$$

The matrix elements in equations 3.6 and 3.8 have similar numerical values. The left-hand side of 3.8 evaluates to 0.619-0.06-0.035-0.016-0.008 = 0.5, which is identical to element(1,1) in equation 3.6. In equation 3.6 the sum of elements (1,6) through (1,10) is 0.805s. The same sum in 3.8 is 0.90s. The small increase in velocity coefficient values, as γ decreases from 0.18 to 0.03, is completely consistent with predictions made by the symbolic analysis.

3.4.3   Framework for Comparison of Control Strategies

In this section we present a simple framework for quantitatively evaluating the similarity between components of response in the time-history analyses.

Scatter Diagram. Figure 3.12 is a symbolic representation of the relationship of two random variables. This statistical evaluation considers the two time history base isolator displacements, D1 and D2, when base isolation (BI) + CKBB and BI+VKBB control is used, respectively. The probability mass density
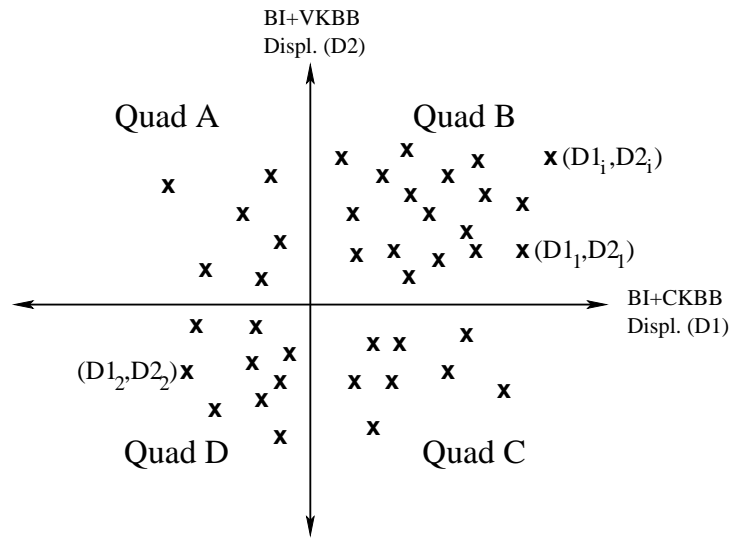
Figure 3.12: Symbolic Representation for Scatter Diagram of Displacement Data Points generated by Control Methodologies 1 and 2. The horizontal axis is base isolation plus constant stiffness bang-bang control (BI+CKBB). The vertical axis is base isolation plus variable stiffness bang-bang control (BI+VKBB).

of (D1, D2) response coordinates can be represented in a scatter diagram. The number of data points in each quadrant of the scatter diagram is shown in Table 3.4.

Correlation Coefficients. The average values of the D1 and D2 are given by:

$$\overline{D1} = \frac{1}{N}\sum_{i=1}^{i=N} D1_i, \quad \overline{D2} = \frac{1}{N}\sum_{i=1}^{i=N} D2_i, \tag{3.9}$$

Measures of variance are given by [18]:

$$\sigma_{D1}^2 = \frac{1}{N}\sum_{i=1}^{i=N} \left(D1_i - \overline{D1}\right)^2. \tag{3.10}$$

$$\sigma_{D2}^2 = \frac{1}{N}\sum_{i=1}^{i=N} \left(D2_i - \overline{D2}\right)^2. \tag{3.11}$$

Measures of co-variance for displacements D1 and D2 are as follows:

$$\mu_{D1D2} = \frac{1}{N}\sum_{i=1}^{i=N} \left(D1_i - \overline{D1}\right) \cdot \left(D2_i - \overline{D2}\right) \tag{3.12}$$

With equations 3.9 through 3.12 in place, the correlation coefficient for "D1 and D2" is as follows:

$$\rho_{D1D2} = \frac{\mu_{D1D2}}{\sigma_{D1}\sigma_{D2}} \tag{3.13}$$

Because the mean square values are always positive, the correlation coefficient will always lie in the interval $[-1, 1]$ (i.e., $-1 < \rho_{D1D2} < 1$). One special case occurs when the variables D1 and D2 are statistically independent; $\mu_{D1D2} = 0$ and, hence, ρ_{D1D1} also equals 0. Based on our symbolic analysis of a simplified 2-DOF system, we expect the displacements, D1 and D2 to be strongly correlated – hence, ρ_{D1D2} should evaluate to a numerical value close to 1. The averages, standard deviations, co-variances, and correlation coefficients are given in Table 3.5.

3.5 Summary of Results

Time history analyses are computed for 20 seconds at discrete intervals of 0.02 seconds. For the time interval $t \in [0, 15]$ seconds the structural system is subject to ground motion excitations plus external actuator forces applied by the control system. From $t \in [15, 20]$ seconds, the dynamic vibration is determined by the actuator forces alone.

Structural Drifts and Base Shear Forces. Figures 3.13 through 3.16 show time histories of structural drifts at the base isolator (node 1) corresponding to the scaled Kobe, San Fernando, Northridge, and Duzce ground motion inputs. Each plot contains contours of displacement for the constant stiffness (i.e., base isolation + CKBB) and variable stiffness (i.e., base isolation + VKBB) control strategies. To benchmark improvements in performance, a third contour for base isolation alone is also shown.

	Base Drift (mm)			Structural Drift (mm)			Base Shear (kN)		
Earthquake	BI	BI+ CKBB	BI+ VKBB	BI	BI+ CKBB	BI+ VKBB	BI	BI+ CKBB	BI+ VKBB
1971 San Fernando	447.60	368.90	368.90	12.38	12.29	12.29	2294.0	1940.0	1940.0
1994 Northridge	206.80	175.30	175.30	9.26	12.86	12.86	1210.0	1068.0	1068.0
1995 Kobe	260.70	203.00	203.00	8.31	10.15	10.15	1453.0	1193.0	1193.0
1999 Duzce	31.13	22.04	22.04	5.43	10.31	10.31	419.3	378.4	378.4

Table 3.3: Simulation Results: Peak Base/Structural Drifts and Base Shears

A summary of peak values in base drift, structural drift, and base shear force for each of the three control cases is given in Table 3.3. It is evident that, on average, peak displacements for constant stiffness bang-bang control (CKBB) are 21% smaller than those occuring for base isolation alone. With the sole exception of the 1971 San Fernando earthquake, CKBB increases structural drift by a modest amount.

51

Earthquake	Quad A	Quad B	Quad C	Quad D	Total
1971 San Fernando	0	198	0	802	1000
1994 Northridge	0	645	0	355	1000
1995 Kobe	0	222	0	778	1000
1999 Duzce	0	270	0	730	1000

Table 3.4: Data Points in Each Quadrant of Scatter Diagram

Earthquake	Avg. D1 (mm)	Avg. D2 (mm)	Std. D1 (mm)	Std. D2 (mm)	Cov. D1,D2 (mm^2)	Corr. D1,D2
1971 San Fernando	-4.58	-4.58	80.61	80.61	6498.00	1
1994 Northridge	4.19	4.19	24.83	24.83	616.60	1
1995 Kobe	-6.13	-6.72	55.03	55.09	3031.00	0.9999
1999 Duzce	-2.29	-2.29	6.01	6.01	36.05	1

Table 3.5: Statistical Comparison of Time-Histories of Displacement. Mesures include average values, standard deviations, covariances, and correlation coefficients

Thus, while active control works to decrease peak lateral displacements at the top of the isolator, these improvements in system performance must be "traded off" against a slight increase in internal forces and element-level displacements within the main structural system.

The summary of statistical metrics in Table 3.5 shows an exact correlation in displacements (i.e., $\rho = 1$) generated by BI+CKBB and BI+VKBB for three of the ground motion inputs, and an extremely strong correlation in displacements generated by the 1995 Kobe earthquake.

The cause-and-effect and sensitivity analysis predictions enabled by symbolic analysis of the two-DOF system (for details, see Section 2.4), correspond well to numerical results from time history analysis of the five-DOF model. Readers should note the domainance of first mode vibrations in both the elastic and inelastic states: ($\Gamma_1 = 1.11$ in the elastic state and $\Gamma_1 = 1.02$ in the inelastic state. For a 2-DOF model with γ varying between $0.03 \leq \gamma \leq 0.18$ and $\tau = 0.00265$ secs^2, Figures 2.7 through 2.9 validate these observations show that there will be very little change in the velocity coefficients of $\mathbf{B}^{\mathbf{T}}\mathbf{S}$.

Nonlinear Force-Displacement Response. Figures 3.17 through 3.20 show time histories of force-displacement in the base isolator (node 1) generated by the scaled Kobe, San Fernando, Northridge, and Duzce ground motion inputs. As expected, peak overall displacements are dominated by the contribution of plastic deformations of the base isolator. The tangent stiffness (i.e., slope of the force-displacement curve) in the pre- and post-yield domains is consistent with the material and section properties described in Section 3.1 and illustrated in Figure 3.2.

Internal Element and Actuator Forces. Figures 3.21 through 3.24 show time histories of internal element forces and actuator forces for system responses generated by the scaled Kobe, San Fernando,
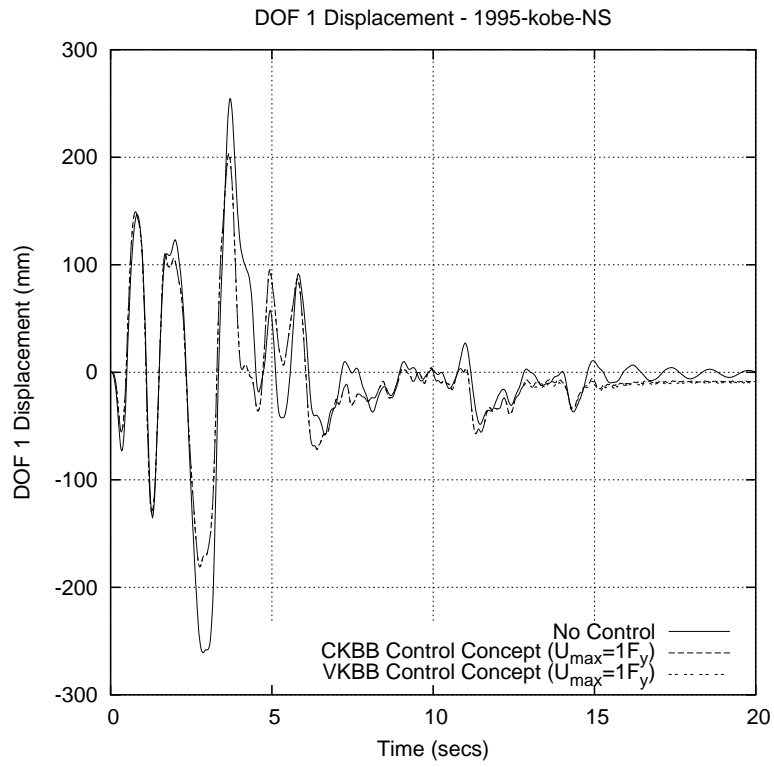
Figure 3.13: CKBB/VKBB Control Comparison: Base Isolator Drift for 1995 Kobe
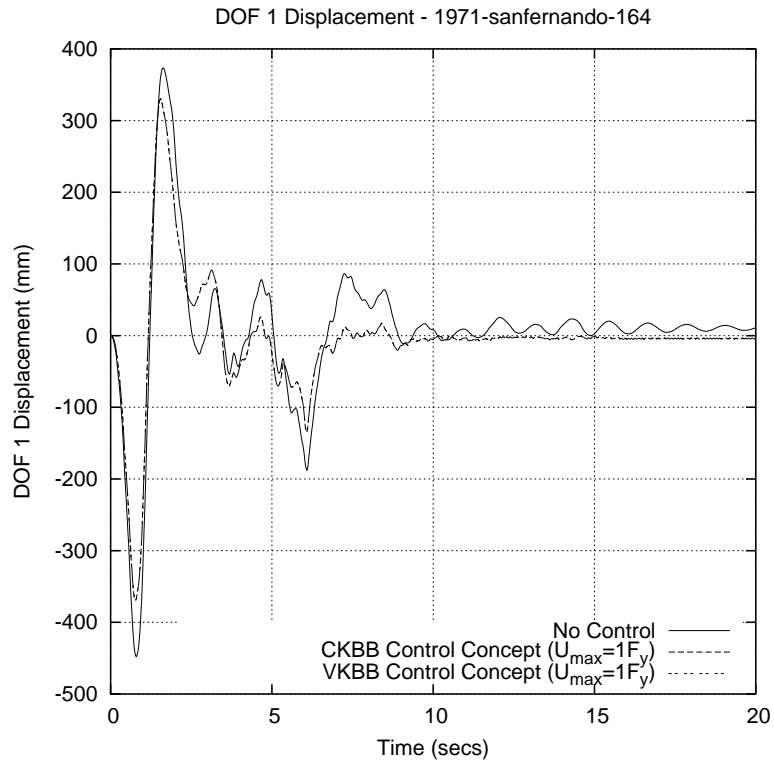
Figure 3.14: CKBB/VKBB Control Comparison: Base Isolator Drift for 1971 San Fernando
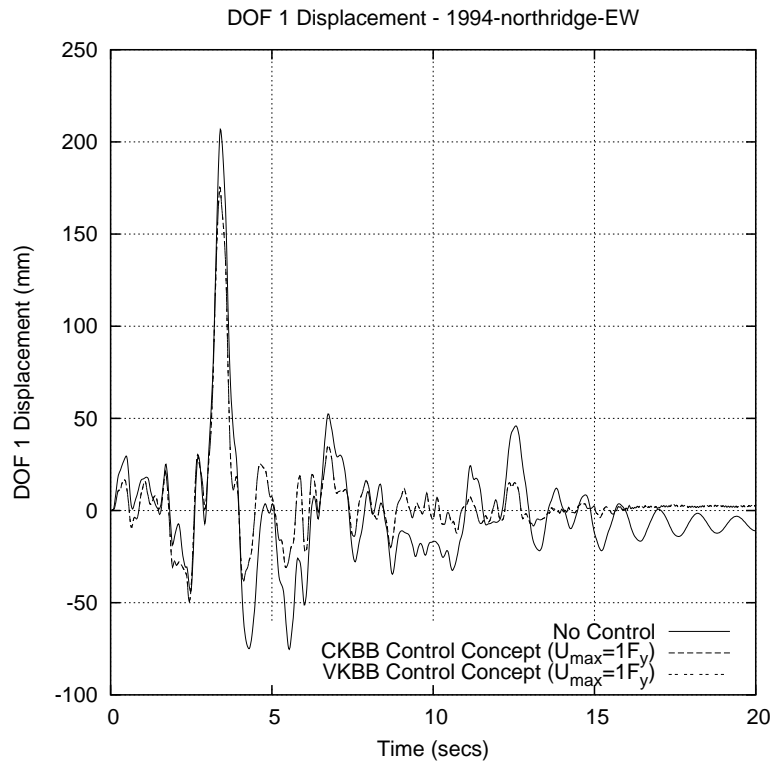
Figure 3.15: CKBB/VKBB Control Comparison: Base Isolator Drift for 1994 Northridge
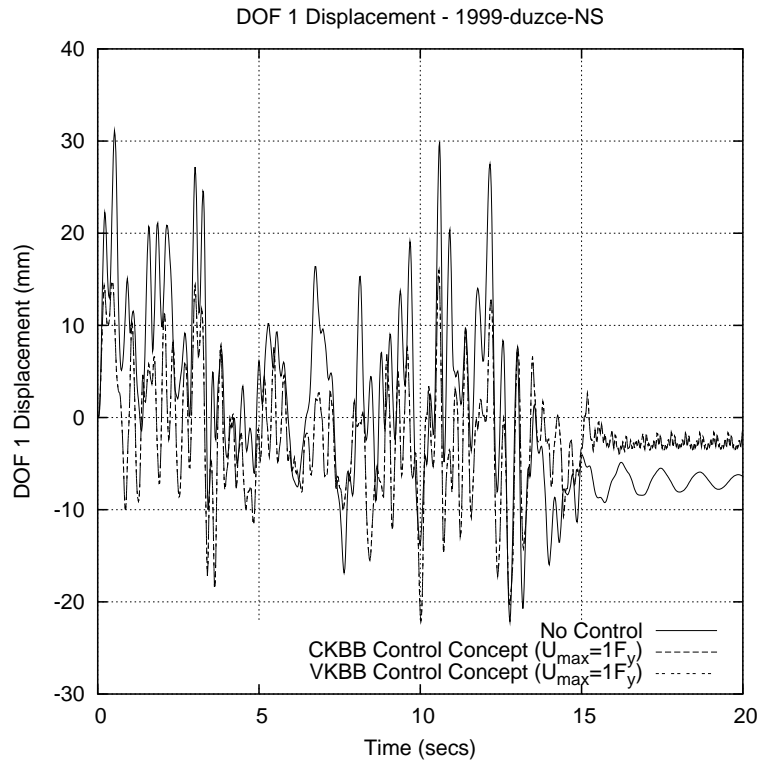
Figure 3.16: CKBB/VKBB Control Comparison: Base Isolator Drift for 1999 Duzce
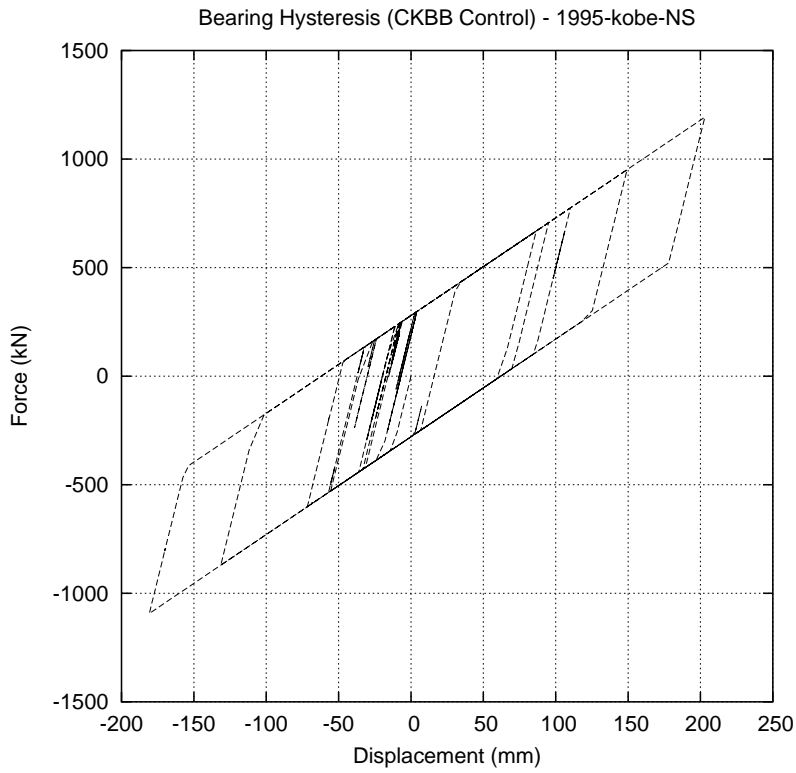
Figure 3.17: Base Isolator Hysteresis: 1995 Kobe.
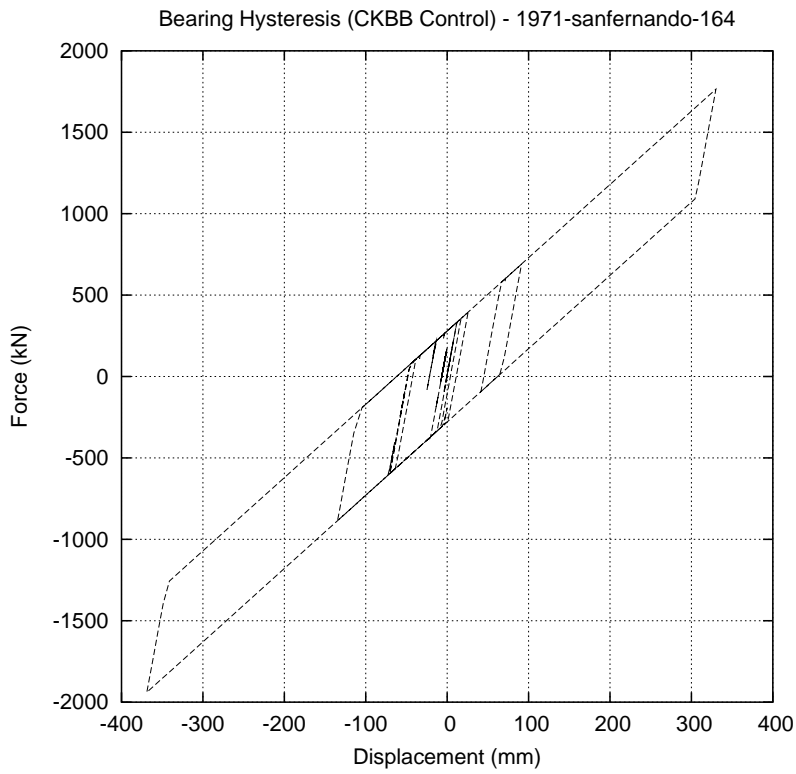
Figure 3.18: Base Isolator Hysteresis: 1971 San Fernando

55
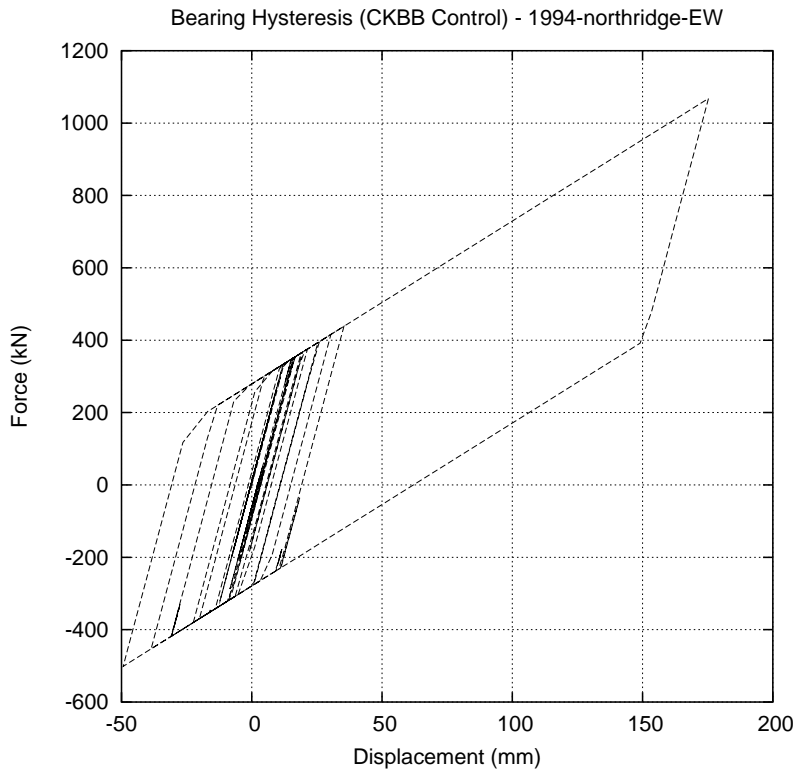
Figure 3.19: Base Isolator Hysteresis: 1994 Northridge
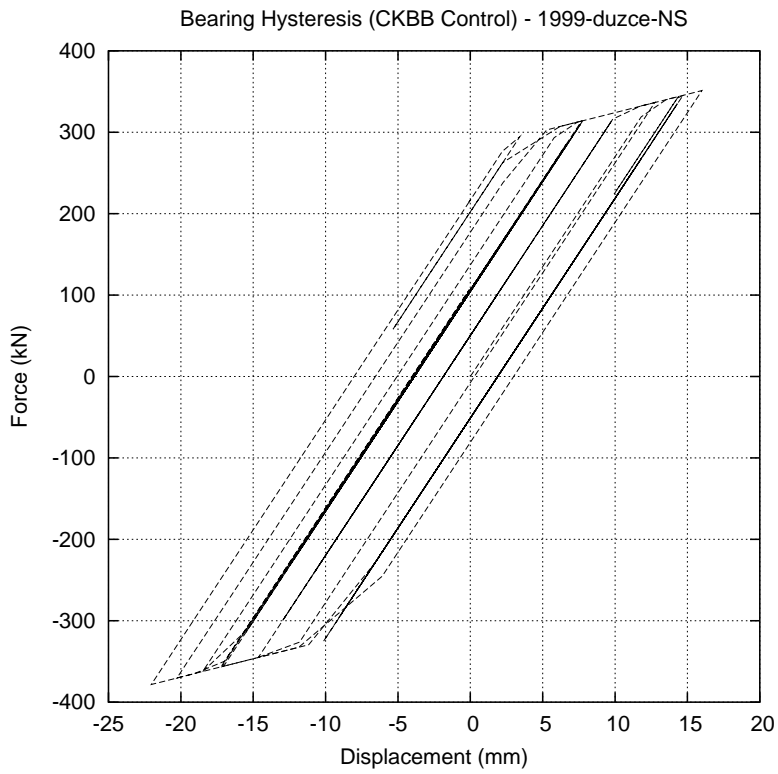
Figure 3.20: Base Isolator Hysteresis: 1999 Duzce

56

Northridge, and Duzce ground motion inputs. In our symbolic analysis for the bang-bang control of a one-degree of freedom system – see Figures 2.1 through 2.3 for the forced vibration case and Figures 2.4 through 2.6 for the free vibration case – we demonstrated that actuator force is "almost in phase" with velocities and and "almost completely out of phase" (i.e., $\pi/2$ radians) with displacements. (This relationship between bang-bang control actuator forces and displacements and velocities is investigated further in a paper by Sebastianelli and Austin [35]). Figures 3.21 and 3.22, in particular, validate this prediction.

Notice, however, that at the end of the displacement-time histories for all the earthquakes, the top of the base isolator oscillates around a zero displacement and the actuator force switches between $\pm u_{max} = 350$ kN at a high frequency. During the "post ground shaking" phase of the time-history response, the actuator adds very little value in terms of reduced displacements and it should be turned off!

Isolator Shear/Actuator Force (CKBB Control) - 1995-kobe-NS
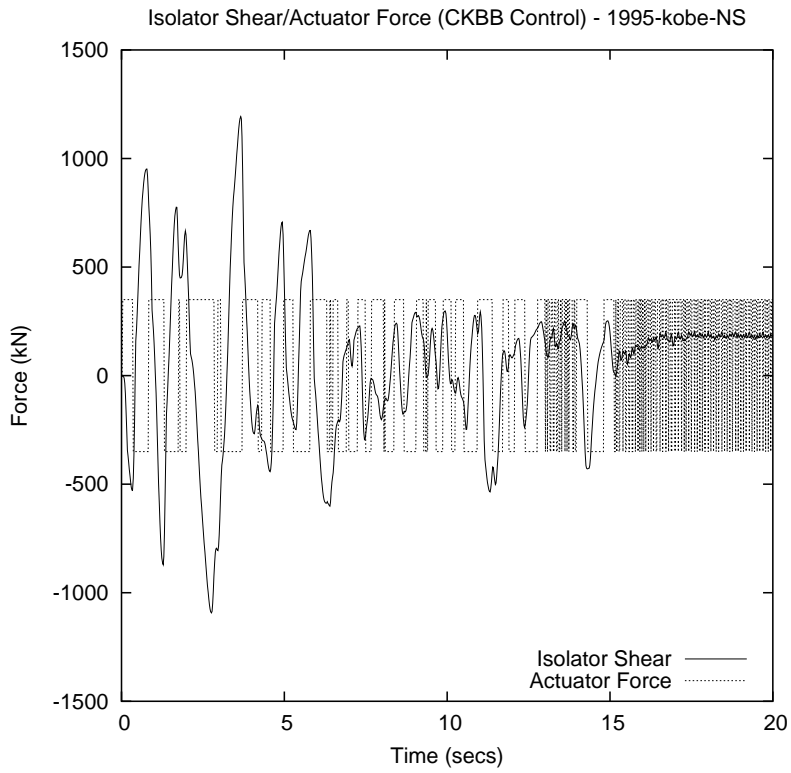
Figure 3.21: Isolator/Actuator Force: 1995 Kobe

Isolator Shear/Actuator Force (CKBB Control) - 1971-sanfernando-164
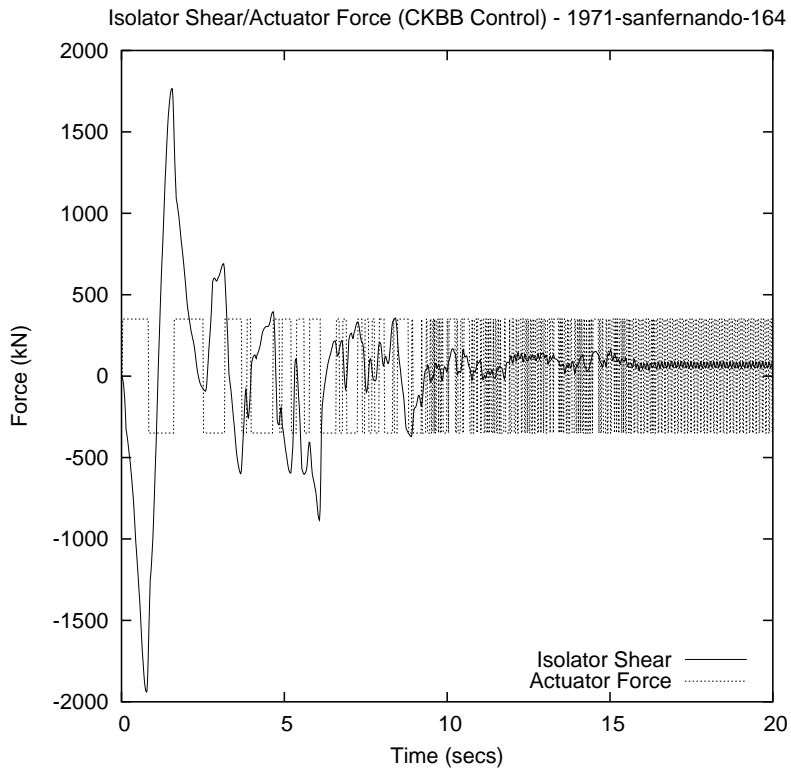
Figure 3.22: Isolator/Actuator Force: 1971 San Fernando

58
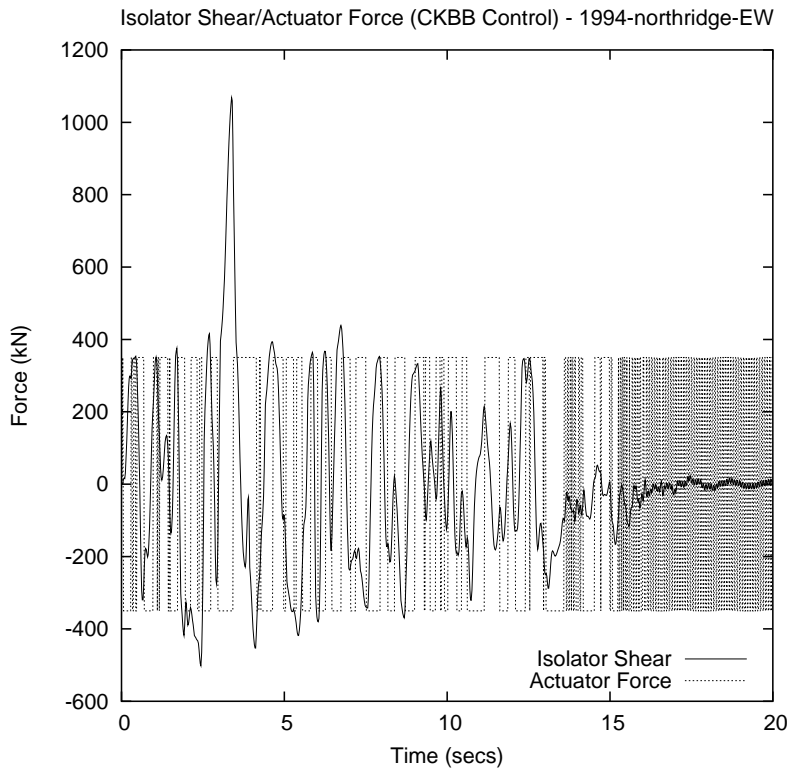
Figure 3.23: Isolator/Actuator Force: 1994 Northridge
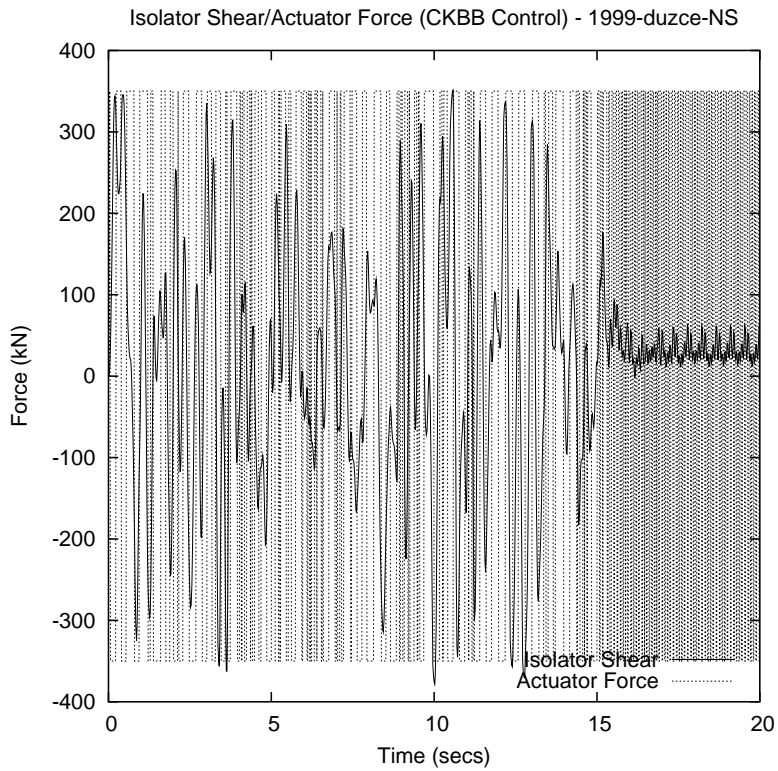
Figure 3.24: Isolator/Actuator Force: 1999 Duzce

59

Chapter 4

Conclusions and Future Work.

4.1   Conclusions

The objective of this study has been to investigate the potential benefits and opportunities for using modified bang-bang control as a supplement to base isolation in the performance-based design of earthquake resistant structures. The work described in this report is simply one step in a long-term research objective aimed at development of analytical procedures and general guidelines to help engineers design structures protected by hybrid passive/active control.

We have employed linear matrix algebra and symbolic analysis software to derive symbolic expressions for bang-bang control, expressed in terms of solutions to the Lyapunov equation, the system parameters (m, k, ...) and state (i.e., displacements and velocities). The investigations included: (1) Symbolic analysis for 1 and 2 DOF systems, (2) Symbolic analysis for n-DOF systems, and (3) Sensitivity analysis of modified bang-bang control to nonlinear deformations in base isolators. Together, the symbolic expressions derived in this study allow for the identication of cause-and-effect relationships between the control algorithm parameters and properties of the dynamical system (e.g., damping matrices), which in turn affects the ensuing system response. Equation 3.2 can be incorporated into equation of motion, 1.1 in a straight-forward manner. Equations 2.70, 2.71 and 2.72 also indicate that if a structure has a stiff superstructure (i.e., low τ) or if a lot of damping (i.e., high ξ) is present then displacements over velocities are more likely to influence this control strategy. We surmise from this observation that "sub-optimal bang-bang control strategies" will be insensitive to localized nonlinearities in the base isolation devices, especially when γ(t) remains within the interval [0.05,0.15]. As such, simplified design procedures might be justified. For design applications where post-yield stiffnesses are very low (i.e., $\min\left(\gamma(t)\right) \approx 0$), the bang-bang control strategy is likely to switch between two modes: (1) a displacement driven strategy for pre-yield states, and (2) a velocity driven strategy for post-yield states. These

observations have been verified via numerical experiments with a nonlinear five-DOF system.

The conclusions of this study are as follows:

1. The numerical simulations suggest that, contrary to initial expectations, the additional complexity associated will nonliear bang-bang control is unwarranted.

   The use of modified bang-bang control algorithms based on linear properties of the structure (i.e., CKBB) results in a displacement-time history response that is superior to bang-bang control algorithms that employ nonlinear state information (i.e., VKBB). The displacement response is superior in terms of reduced peak displacements and a best effort to ensure displacements osillate around zero.

   VKBB is more difficult to incorporate into the equation of motion since the control algorithm is dependant on the linear or nonlinear state of the structure. Moreover, nonlinear modified bang-bang control results in a displacement time history that is not a best effort to oscillate around zero, and for this reason the control objective of nonlinear modified bang-bang control has less physical intuition, and less amenable to practitioners, than the control ojective of its linear counterpart. These observations provide justification for using the simplified linear modified bang-bang control scheme, with the control parameters $a = b = 1$ without a significant loss of accuaracy.

2. The control algorithm is sensitive to the selection of $\mathbf{Q}$ and therefore the terms in $\mathbf{Q}$ should not be selected as relative, arbitary values. Time history responses of displacement for the simulation cases (a=1, b=0) and (a=1, b=1) are almost identical. For details, see Figure **??**. Minimization of potential energy in the superstructure alone (a=0, b=1) results in a displacement-time history that is inferior to either of the former two cases.

3. Underlying "cause and effect" relationships of linear modified bang-bang control are better understood. For instance, the effect of how the mass/stiffness ratio (τ) of the superstructure and damping model used and damping ratio (ξ) are better understood.

4.2   Future Work

Throughout this study we have employed simplifying assumptions to facilitate insight into cause-and-effect relationships and numerical studies. An underlying assumption of this work is that

present-day technology is capable of delivering the actuator force and reach consistent with levels predicted by the analysis. This work also assumes that present-day technology would be capable of satisfying the associated power requirements. The energy-balance analysis of Austin and Lin needs to be extended to a power-balance framework, thereby creating a quantitative framework for assessing the validity of these assumptions.

In moving from symbolic analysis and prototype-level numerical studies to a full-scale experimental study, several of these assumptions would need to be re-examined. They include:

1. **Singular Control-Force Delivery Requirement.** Since bang-bang control laws lead to a singular control-force delivery requirement, servohydraulic actuators are not suitable for this kind of control law due to high-speed switching of control forces that are needed to meet this requirement. Therefore, modification is necessary for practical application of bang-bang control laws to civil engineering structures. Wu and Soong [43] propose a method of approximating this singular control requirement using series of polynomial functions. Therefore a discontinuous function, such as the control-force delivery requirement for bang-bang control may be approximated as a series of polynomials as proposed by Wu and Soong [43].

2. **Availability of State Variables.** In this study, it is assumed that the state variables i.e., the displacements and velocities at each degree of freedom are readily measurable. The bang-bang control algorithm is dependent on the availability of the state variables, (see equation 1.14). Dyke et al. [20] points out that accurate measurement of displacements and velocities is difficult to achieve since during a seismic event the foundation of the structure is moving with the ground. It is suggested that since accelerometers are readily available and an inexpensive measurement of accelerations at strategic points on the structure is an ideal solution to this problem. Also, Chung et al. [16] point out that the error in the observability of these state variables along with structural controllability issues and on-line computational errors tend to accumulate rapidly and may degrade the structural performance seriously or produce instability.

3. **Time Delay.** In the analyses presented in this study, time delay is not taken into account; however, time delay between the measured variables and the application of the control forces can not be eliminated. Chung et al. [16] points out that time lag diminished control effects for a real system as compared to an ideal one. Since phase lag is proportional to time delay and modal frequency, the effect of time delay may be very serious for higher modes even with small amounts of time delay. Chung et al. [16, 17] developed a phase shift method for SDOF systems which compensates

for time delay in the modal domain.

4. **Actuator Location.** In the derivations and numerical experiment in this study, a single actuator is located at the top of the base isolator (DOF 1). The reasoning for the location of this actuator is that for base isolated structures the main potential benefit is believed to lie in the ability of active control to limit the maximum base displacement while the base isolation limits interstory drift and absolute acceleration [23]. Brown, Ankireddi, and Yang [12], studied the problem of actuator and sensor placement for multiobjective control. A linear quadratic Gaussian control algorithm that synthesizes Pareto optimal trade-off curves was used to determine the optimal location of actuators and sensors in this parametric study. Cheng and Jiang [14] used a statistical method for determining the optimal placement of control devices and showed that optimal placement of control devices resulted in better performance because less control force was required to reduce structural seismic response to a given level.

In a few of our computer simulations the post-earthquake phase of the system response has been completely dominated by the actuator system. Our hope is that the power-balance analysis, coupled with a simple strategy for adapting U_{max} will mitigate this problem by simply turning the active control off!

4.3   Acknowledgments.

Bibliography

[1] AASHTO. *Guide Specifications for Seismic Isolation Design*. 1991.

[2] Andriono T., Carr A.J. A Simplified Earthquake Resistant Design Method for Base Isolated MultiStorey Buildings. *Bulletin of the New Zealand National Society for Earthquake Engineering*, 24(3):238–250, September 1991.

[3] Andriono T., Carr A.J. Reduction and Distribution of Lateral Seismic Forces on Base Isolated Mutli-Storey Structures. *Bulletin of the New Zealand National Society for Earthquake Engineering*, 24(3):225–237, September 1991.

[4] Arias A. *A Measure of Earthquake Intensity in Seismic Design for Nuclear Power Plants*. MIT Press, 1970. Hansen R., ed.

[5] Austin M. A., and Lin W. J. Energy-Balance Assessment of Isolated Structures. *Journal of Engineering Mechanics*, 130(3):347–358, 2003.

[6] Austin M. A., Lin W. J., and Chen X. G. Structural Matrix Computations with Units. *Journal of Computing in Civil Engineering*, 14(3):174–182, 2000.

[7] Austin M. A., Chen X. G., Lin W-J. ALADDIN: A Computational Toolkit for Interactive Engineering Matrix and Finite Element Analysis. Technical Report TR95-74, Institute for Systems Research, University of Maryland, College Park, December 1995.

[8] Austin M. A., Pister K. S., Mahin S. A. A Methodology for the Probabilistic Limit States Design of Earthquake Resistant Structures. *Journal of the Structural Division, ASCE*, 113(8):1642–1659, August 1987.

[9] Austin M. A., Pister K. S., Mahin S. A. Probabilistic Limit States Design of Moment Resistant Frames Under Seismic Loading. *Journal of the Structural Division, ASCE*, 113(8):1660–1677, August 1987.

[10] Belanger P. R. *Control Engineering : A Modern Approach*. Saunders College Publishing, Fort Worth, TX, 1995.

[11] Bellman R., Glicksberg I., and Gross O. On the Bang-Bang Control Problem. *Quarterly of Applied Mathematics*, 14(1):11–18, 1956.

[12] Brown A. S., Ankireddi S., and Yang H. T. Actuator and Sensor Placement For Multiobjective Control of Structures. *Journal of Structural Engineering*, 125(7):757–765, 1999.

[13] Cai G., Huang J., Sun, F., and Wang C. Modified Sliding-Mode Bang-Bang Control for Seismically Excited Linear Structures. *Earthquake Engineering and Structural Dynamics*, 29.

[14] Cheng F. Y. and Jiang H. Hybrid Control of Seismic Structures with Optimal Placement of Control Devices. *Journal of Aerospace Engineering*, 11(2):52–58, 1998.

[15] Chopra A. K. *Dynamics of Structures: Theory and Applications to Earthquake Engineering*. Prentice Hall, 1995.

[16] Chung L. L., Lin R. C., Soong T. T., and Reinhorn A. M. Experimental Study of Active Control for MDOF Seismic Structures. *Journal of Engineering Mechanics*, 115(8):1609–1627, 1989.

[17] Chung L. L., Reinhorn A. M., and Soong T. T. Experiments on Active Control of Seismic Structures. *Journal of Engineering Mechanics*, 114:241–256, 1988.

[18] Clough R. W., Penzien J. *Dynamics of Structures*. McGraw-Hill, New York, New York, 1993.

[19] Connor J.J. *Introduction to Structural Motion Control*. Pearson Education, Inc., 2003.

[20] Dyke S. J., Spencer B. F., Jr., Quast P., Sain M. K., Kaspari D. C., and Soong T. T. Acceleration Feedback Control of MDOF Structures. *Journal of Engineering Mechanics*, 122(9):907–918, 1996.

[21] Earthquake Engineering Research Center, UC Berkeley. Pacific Earthquake Engineering Research (PEER) Strong Motion Database. *http://peer.berkeley.edu/smcat/index.html*.

[22] Ghobarah A., Ali H.M. Seismic Design of Base-Isolated Highway Bridges utilizing Lead-Rubber Bearings. *Canadian Journal of Civil Engineering*, 17:413–422, 1990.

[23] Housner G. W., Bergman L. A., et al. Structural Control: Past, Present, and Future. *Journal of Engineering Mechanics*, 123(9):897–971, 1997.

[24] Johnson E. A., Ramallo J. C., Spencer B. F., Jr., and Sain M. K. Intelligent Base Isolation Systems. In *Proceedings of the Second World Conference on Structural Control*, 1998.

[25] Kailath T. *Linear Systems*. Prentice-Hall, London, England, 1980.

[26] Kayen R. E. and Mitchell J. K. Variation of the Intensity of Earthquake Motion Beneath the Ground Surface. In *Proceeding of the Sixth National Conference on Earthquake Engineering*, 1998. Seattle, May 31 - June 4.

[27] Lin W. J. Modern Computational Environments for Seismic Analysis of Highway Bridge Structures, 1997. Doctoral Dissertation.

[28] Makris N. Rigidity-Plasticity-Viscosity : Can Electrorheological Dampers Protect Base-Isolated Structures from Near-Source Earthquakes. *Journal of Engineering and Structural Dynamics*, 26:571–591, 1997.

[29] Mayes R.L., Buckle I.G., Kelly T.R., Jones L. AASHTO Seismic Isolation Design Requirements for Highway Bridges. *Journal of the Structural Division, ASCE*, 118(1):284–304, January 1992.

[30] Naeim F. and Kelly J. *Design of Seismic Isolated Structures*. John Wiley and Sons, 1998.

[31] Newmark N.M., Hall W.J. *Earthquake Spectra and Design. A Primer*. Earthquake Research Institute, Berkeley, CA, 1982.

[32] Park J. and Otsuka H. Optimal Yield Level of Bilinear Seismic Isolation Devices. *Earthquake Engineering and Structural Dynamics*, 28.

[33] Reinhorn A. M., Soong T. T., and Wen C. Y. Base-isolated Structures with Active Control. In *Proceedings of Pressure Vessels and Piping (PVP) Conference*, volume PVP-127, pages 413–420, 1987.

[34] Robinson W. H. Lead-Rubber Hysteretic Bearings Suitable for Protecting Structures During an Earthquake. *Earthquake Engineering and Structural Dynamics*, 10:593–602, 1982.

[35] Sebastianelli R. R., Jr., and Austin M. A. Phase Analysis of Actuator Response of Semi-Active Bang-Bang Control of Base Isolated Structures. *Earthquake Engineering and Structural Dynamics in press*.

[36] Skinner R. I., Robinson W. H., McVerry G. H. *An Introduction to Seismic Isolation*. John Wiley & Sons, Inc., 1993.

[37] Spencer B. F., Jr. and Nagarajaiah S. State of the Art of Structural Control. *Journal of Structural Engineering*, pages 845–856, July 2003.

[38] *Dynamic Structural Design : An Inverse Approach*. WIT Press, 2000.

[39] Turkington D.H., Carr A.J., Cooke N., and Moss P.J. Design Method for Bridges on Lead-Rubber Bearings. *Journal of the Structural Division, ASCE*, 115(12):3017–3030, December 1989.

[40] Turkington D.H., Carr A.J., Cooke N., and Moss P.J. Seismic Design of Bridges on Lead-Rubber Bearings. *Journal of the Structural Division, ASCE*, 115(12):3000–3016, December 1989.

[41] Tyler R.G. Rubber Bearings in Base Isolated Structures : A Summary Paper. *Bulletin of the New Zealand National Society of Earthquake Engineering*, 24(3), September 1991.

[42] Wonham W. M. and Johnson C. D. Optimal Bang-Bang Control with Quadratic Performance Index. *Journal of Basic Engineering*, 86:107–115, 1964.

[43] Wu Z., and Soong T. T. Modified Bang-Bang Control Law for Structural Control Implementation. *Journal of Engineering Mechanics*, 122(8):771–777, 1996.

[44] Wu Z., Soong T. T., Gattulli V., and Lin R. C. Nonlinear Control Algorithms for Peak Response Reduction. Technical Report NCEER-95-0004, National Center for Earthquake Engineering Research, State University of New York at Buffalo, Buffalo, NY. 14261, February 1995.

[45] Yoshioka H., Ramallo J. C., and Spencer B. F., Jr. Smart Base Isolation Strategies Employing Magnetorheological Dampers. *Journal of Engineering Mechanics*, 128(5):540–551, 2002.

Appendix A

Scalability of Solutions to the Lyapunov Matrix Equation

The following matrix equations prove that when the total potential energy and/or kinetic energy of a structure is minimized, under certain restrictions on the form of the mass, damping, and stiffness matrices, the solution to the Lyapunov matrix equation for a 1-DOF system is scalable to an n-DOF system. These restrictions on the form of the mass, damping, and stiffness matrices are as follows:

1. The mass matrix, $\mathbf{M}$, must be diagonal and uniform (i.e., $m_1 = m_2 = ... = m_n$).

2. Linear viscous damping (in the form $\alpha \cdot \mathbf{M} + \beta \cdot \mathbf{K}$) must be present in the system.

3. The structural stiffness matrix, $\mathbf{K}$, must be well-conditioned.

Consider a 1-DOF system with stiffness, k, mass, m, and linear viscous damping, c= $\alpha \cdot m + \beta \cdot k$. For the following general choice of $\mathbf{Q}$,

$$\mathbf{Q} = \begin{bmatrix} k^\star & 0 \\ 0 & 0 \end{bmatrix}, \tag{A.1}$$

where $k^\star$ is a real, positive number, the solution to the Lyapunov matrix equation for $\mathbf{S}$ is as follows:

$$\mathbf{S} = \begin{bmatrix} \frac{mk^\star}{2(\alpha \cdot m + \beta \cdot k)} + \frac{(\alpha \cdot m + \beta \cdot k)k^\star}{2k} & \frac{mk^\star}{2k} \\ \frac{mk^\star}{2k} & \frac{m^2 k^\star}{2k(\alpha \cdot m + \beta \cdot k)} \end{bmatrix}. \tag{A.2}$$

Substituting equation 1.4 (the defination for $\mathbf{A}$) into the matrix equation $\mathbf{A}^{\mathbf{T}}\mathbf{S} + \mathbf{S}\mathbf{A} = -\mathbf{Q}$, and noting that $\mathbf{K}^{\mathbf{T}} = \mathbf{K}$ and $\mathbf{M}^{\mathbf{T}} = \mathbf{M}$, we have:

$$\mathbf{A}^{\mathbf{T}}\mathbf{S} + \mathbf{S}\mathbf{A} = \begin{bmatrix} \mathbf{0} & -([\mathbf{K}][\mathbf{M^{-1}}]) \\ [\mathbf{I}] & -([\mathbf{C}][\mathbf{M^{-1}}]) \end{bmatrix} \mathbf{S} + \mathbf{S} \begin{bmatrix} \mathbf{0} & [\mathbf{I}] \\ -([\mathbf{M^{-1}}][\mathbf{K}]) & -([\mathbf{M^{-1}}][\mathbf{C}]) \end{bmatrix} = -\mathbf{Q}. \tag{A.3}$$

Now notice that the matrix elements of equation A.2 are symbolic expressions expressed as fractions. For the matrix counterpart of equation A.2, one can either pre- or post-multiply the matrix expression appearing as the denuminator of each matrix element. We investigate both scenarios to ascertain if, and under what conditions, the symbolic form for the SDOF system will scale to a MDOF system.

A.1 Pre-Multiplication Matrix Strategy for S

Using pre-multiplication to calculate the matrix $\mathbf{S}$ (see equation A.2) and substituting the analogous matrix equation of equation A.2 into equation A.3, gives the following results:

A.1.1 Matrix Product $\mathbf{A}^T\mathbf{S}$:

$$\text{Element 1-1} = -\frac{1}{2}[\mathbf{K}^{-1}][\mathbf{K}][\mathbf{K}^\star] = -\frac{1}{2}[\mathbf{K}^\star] \tag{A.4}$$

$$\text{Element 1-2} = -\frac{1}{2}[\mathbf{K}][\mathbf{M}^{-1}][\mathbf{K}^{-1}][\mathbf{C}^{-1}][\mathbf{M}][\mathbf{M}][\mathbf{K}^\star] \tag{A.5}$$

$$\text{Element 2-1} = \frac{1}{2}[\mathbf{C}^{-1}][\mathbf{M}][\mathbf{K}^\star] + \frac{1}{2}[\mathbf{K}^{-1}][\mathbf{C}][\mathbf{K}^\star] - \frac{1}{2}[\mathbf{C}][\mathbf{M}^{-1}][\mathbf{K}^{-1}][\mathbf{M}][\mathbf{K}^\star] \tag{A.6}$$

$$\text{Element 2-2} = \frac{1}{2}[\mathbf{K}^{-1}][\mathbf{M}][\mathbf{K}^\star] - \frac{1}{2}[\mathbf{C}][\mathbf{M}^{-1}][\mathbf{K}^{-1}][\mathbf{C}^{-1}][\mathbf{M}][\mathbf{M}][\mathbf{K}^\star] \tag{A.7}$$

A.1.2 Matrix Product $\mathbf{S}\mathbf{A}$:

$$\text{Element 1-1} = -\frac{1}{2}[\mathbf{K}^{-1}][\mathbf{M}][\mathbf{K}^\star][\mathbf{M}^{-1}][\mathbf{K}] \tag{A.8}$$

$$\text{Element 1-2} = \frac{1}{2}[\mathbf{C}^{-1}][\mathbf{M}][\mathbf{K}^\star] + \frac{1}{2}[\mathbf{K}^{-1}][\mathbf{C}][\mathbf{K}^\star] - \frac{1}{2}[\mathbf{K}^{-1}][\mathbf{M}][\mathbf{K}^\star][\mathbf{C}][\mathbf{M}^{-1}] \tag{A.9}$$

$$\text{Element 2-1} = -\frac{1}{2}[\mathbf{K}^{-1}][\mathbf{C}^{-1}][\mathbf{M}][\mathbf{M}][\mathbf{K}^\star][\mathbf{K}][\mathbf{M}^{-1}] \tag{A.10}$$

$$\text{Element 2-2} = \frac{1}{2}[\mathbf{K}^{-1}][\mathbf{M}][\mathbf{K}^\star] - \frac{1}{2}[\mathbf{K}^{-1}][\mathbf{C}^{-1}][\mathbf{M}][\mathbf{M}][\mathbf{K}^\star][\mathbf{C}][\mathbf{M}^{-1}] \tag{A.11}$$

It is easy to see that when $[\mathbf{K}^\star] = [\mathbf{K}]$ and $[\mathbf{M}]$ is diagonal and uniform (i.e., $m_1 = m_2 = \ldots = m_n$) equations A.4 through A.11 simplify. Substituting $[\mathbf{K}^\star] = [\mathbf{K}]$ into equations A.4 through A.11, assuming a diagonal and uniform mass matrix, $[\mathbf{M}]$, and substituting this resultant into equation A.3 results in the following:

$$\mathbf{A^T S + SA} = \left[\begin{array}{cc} -[\mathbf{K}] & 0 \\ \left(\begin{array}{c} \frac{1}{2}[\mathbf{C^{-1}}][\mathbf{M}][\mathbf{K}] + \frac{1}{2}[\mathbf{K^{-1}}][\mathbf{C}][\mathbf{K}] \\ -\frac{1}{2}[\mathbf{C}] - \frac{1}{2}[\mathbf{K^{-1}}][\mathbf{C^{-1}}][\mathbf{M}][\mathbf{K}][\mathbf{K}] \end{array} \right) & \left(\begin{array}{c} [\mathbf{K^{-1}}][\mathbf{M}][\mathbf{K}] - \frac{1}{2}[\mathbf{C}][\mathbf{K^{-1}}][\mathbf{C^{-1}}][\mathbf{M}][\mathbf{K}] \\ -\frac{1}{2}[\mathbf{K^{-1}}][\mathbf{C^{-1}}][\mathbf{M}][\mathbf{K}][\mathbf{C}] \end{array} \right) \end{array} \right],$$

$$(A.12)$$

Note the following equalities:

1. $[\mathbf{K^{-1}}][\mathbf{C}][\mathbf{K}] = [\mathbf{C}]$

2. $[\mathbf{K^{-1}}][\mathbf{C^{-1}}][\mathbf{M}][\mathbf{K}] = [\mathbf{C^{-1}}][\mathbf{M}]$

3. $[\mathbf{C}][\mathbf{K^{-1}}][\mathbf{C^{-1}}] = [\mathbf{K^{-1}}]$

4. $[\mathbf{C^{-1}}][\mathbf{M}][\mathbf{K}][\mathbf{C}] = [\mathbf{M}][\mathbf{K}]$

Substituting these equalities into equation A.12 and simplifying terms gives:

$$\mathbf{A^T S + SA} = \left[\begin{array}{cc} -[\mathbf{K}] & \mathbf{0} \\ \mathbf{0} & \mathbf{0} \end{array} \right] = -\mathbf{Q}. \tag{A.13}$$

A.2   Post-Multiplication Matrix Strategy for S

Using post-multiplication to calculate the matrix $\mathbf{S}$ (see equation A.2) and substituting the analogous matrix equation of equation A.2 into equation A.3, gives the following results:

A.2.1   Matrix Product $\mathbf{A^T S}$:

$$\text{Element 1-1} = -\frac{1}{2}[\mathbf{K}][\mathbf{K^\star}][\mathbf{K^{-1}}] \tag{A.14}$$

$$\text{Element 1-2} = -\frac{1}{2}[\mathbf{K}][\mathbf{M}][\mathbf{K^\star}][\mathbf{K^{-1}}][\mathbf{C^{-1}}] \tag{A.15}$$

$$\text{Element 2-1} = \frac{1}{2}[\mathbf{M}][\mathbf{K^\star}][\mathbf{C^{-1}}] \tag{A.16}$$

$$\text{Element 2-2} = \frac{1}{2}[\mathbf{M}][\mathbf{K^\star}][\mathbf{K^{-1}}] - \frac{1}{2}[\mathbf{C}][\mathbf{M}][\mathbf{K^\star}][\mathbf{K^{-1}}][\mathbf{C^{-1}}] \tag{A.17}$$

A.2.2   Matrix Product $\mathbf{SA}$:

$$\text{Element 1-1} = -\frac{1}{2}[\mathbf{M}][\mathbf{K^\star}][\mathbf{K^{-1}}][\mathbf{M}][\mathbf{K}] \tag{A.18}$$

$$\text{Element 1-2} = \frac{1}{2}[\mathbf{M}][\mathbf{K}^{\star}][\mathbf{C}^{-1}] + \frac{1}{2}[\mathbf{C}][\mathbf{K}^{\star}][\mathbf{K}^{-1}] - \frac{1}{2}[\mathbf{M}][\mathbf{K}^{\star}][\mathbf{K}^{-1}][\mathbf{M}^{-1}][\mathbf{C}] \qquad \text{(A.19)}$$

$$\text{Element 2-1} = -\frac{1}{2}[\mathbf{M}][\mathbf{M}][\mathbf{K}^{\star}][\mathbf{K}^{-1}][\mathbf{C}^{-1}][\mathbf{M}^{-1}][\mathbf{K}] \qquad \text{(A.20)}$$

$$\text{Element 2-2} = \frac{1}{2}[\mathbf{M}][\mathbf{K}^{\star}][\mathbf{K}^{-1}] - \frac{1}{2}[\mathbf{M}][\mathbf{M}][\mathbf{K}^{\star}][\mathbf{K}^{-1}][\mathbf{C}^{-1}][\mathbf{M}^{-1}][\mathbf{C}] \qquad \text{(A.21)}$$

As with the pre-multiplication strategy for calculating $\mathbf{S}$, when $[\mathbf{K}^{\star}] = [\mathbf{K}]$ and $[\mathbf{M}]$ is diagonal and uniform (i.e., $m_1 = m_2 = \ldots = m_n$) equations A.14 through A.21 simplify. Substituting $[\mathbf{K}^{\star}] = [\mathbf{K}]$ into equations A.14 through A.21, assuming a diagonal and uniform mass matrix, $[\mathbf{M}]$, and substituting this resultant into equation A.3 results in the following:

$$\mathbf{A}^{\mathbf{T}}\mathbf{S} + \mathbf{S}\mathbf{A} = \begin{bmatrix} -[\mathbf{K}] & -\frac{1}{2}[\mathbf{K}][\mathbf{M}][\mathbf{C}^{-1}] + \frac{1}{2}[\mathbf{M}][\mathbf{K}][\mathbf{C}^{-1}] \\ \frac{1}{2}[\mathbf{M}][\mathbf{K}][\mathbf{C}^{-1}] - \frac{1}{2}[\mathbf{M}][\mathbf{C}^{-1}][\mathbf{K}] & \frac{1}{2}[\mathbf{M}] - \frac{1}{2}[\mathbf{C}][\mathbf{M}][\mathbf{C}^{-1}] \end{bmatrix}. \qquad \text{(A.22)}$$

Note the following equalities:

1. $[\mathbf{K}][\mathbf{C}^{-1}] = ([\mathbf{K}][\mathbf{C}^{-1}])^{\mathbf{T}} = [\mathbf{C}]^{\mathbf{T}}[\mathbf{K}]^{\mathbf{T}} = [\mathbf{C}^{-1}][\mathbf{K}]$

2. $[\mathbf{C}][\mathbf{M}][\mathbf{C}^{-1}] = [\mathbf{M}]$

3. $[\mathbf{K}][\mathbf{M}] = ([\mathbf{K}][\mathbf{M}])^{\mathbf{T}} = [\mathbf{M}]^{\mathbf{T}}[\mathbf{K}]^{\mathbf{T}} = [\mathbf{M}][\mathbf{K}]$

Substituting these equalities into equation A.22 and simplifying terms gives:

$$\mathbf{A}^{\mathbf{T}}\mathbf{S} + \mathbf{S}\mathbf{A} = \begin{bmatrix} -[\mathbf{K}] & \mathbf{0} \\ \mathbf{0} & \mathbf{0} \end{bmatrix} = -\mathbf{Q}. \qquad \text{(A.23)}$$

Appendix B

Notation

The following symbols are used in this paper:

A = cross section area of structural element;

a = damping matrix coefficients;

$\mathbf{C}$ = viscous damping matrix;

E = Young's Modulus of Elasticity;

F(.) = (n × 1) vector of straining and damping forces;

f_y = yield force;

g = acceleration due to gravity;

I = moment of inertia;

J = energy (Joules);

$\mathbf{K}$ = global stiffness matrix;

k = element-level stiffness matrix;

L = length of beam element;

$\mathbf{M}$ = mass matrix;

n = number of degrees of freedom in global structural model;

R(.) = (n × 1) vector of general forces, and, (n × 1) vector of residual forces in (nonlinear) Newmark
    integration;

$\mathbf{r}$ = (n × 1) vector describing the movement of each structural degree of freedom due to a unit ground displacement;

T = kinetic energy, and, natural period of vibration;

t = time (sec);

$t*$ = time (sec) after structural vibrations have completely stopped;

$u(t)$ = (n × 1) vector of displacements at structural degrees of freedom;

$\dot{u}(t)$ = (n × 1) vector of velocities at structural degrees of freedom;

$\ddot{u}(t)$ = (n × 1) vector of accelerations at structural degrees of freedom;

W = work done by internal/external loads;

β = Newmark parameter;

γ = Newmark parameter;

τ = time (sec);

$\triangle t$ = time increment in Newmark integration.

Subscripts:

damping = damping forces;

e = elastic stiffness matrix;

eff = effective stiffness and effective mass;

ext = external loads;

g = ground motion;

int = internal loads;

straining = straining forces;

t = tangent stiffness matrix, and, total displacement, velocity, or acceleration;

1,2 = damping matrix coefficients.